

Connection between asymptotic normalization coefficients and resonance widths of mirror states

A. M. Mukhamedzhanov

Cyclotron Institute, Texas A&M University, College Station, Texas 77843, USA



(Received 24 September 2018; revised manuscript received 22 December 2018; published xxxxxx)

Asymptotic normalization coefficients (ANCs) are fundamental nuclear constants that play an important role in nuclear reactions, nuclear structure, and nuclear astrophysics. In this paper a connection between ANCs and resonance widths of the mirror states is established. Using the Pinkston-Satchler equation the ratio for resonance widths and ANCs of mirror nuclei is obtained in terms of the Wronskians from the radial overlap functions and regular solutions of the two-body Schrödinger equation with the short-range interaction excluded. This ratio allows one to use microscopic overlap functions for mirror nuclei in the internal region, where they are the most accurate, to correctly predict the ratio of the resonance widths and ANCs for mirror nuclei, which determine the amplitudes of the tails of the overlap functions. If the microscopic overlap functions are not available one can express the Wronskians for the resonances and mirror bound states in terms of the corresponding mirror two-body potential-model wave functions. A further simplification of the Wronskian ratio leads to the equation for the ratio of the resonance widths and mirror ANCs, which is expressed in terms of the ratio of the two-body Coulomb scattering wave functions at the resonance energy and at the binding energy [N. K. Timofeyuk, R. C. Johnson, and A. M. Mukhamedzhanov, *Phys. Rev. Lett.* **91**, 232501 (2003)]. Calculations of the ratios of resonance widths and mirror ANCs for different nuclei are presented. From this ratio one can determine the resonance width if the mirror ANC is known and vice versa. Comparisons with available experimental ratios are done.

DOI: [10.1103/PhysRevC.00.004300](https://doi.org/10.1103/PhysRevC.00.004300)

I. INTRODUCTION

The asymptotic normalization coefficient (ANC) is a fundamental nuclear characteristic of bound states [1,2], playing an important role in nuclear reaction and structure physics. The ANCs determine the normalization of the peripheral part of transfer reaction amplitudes [1,2] and overall normalization of the peripheral radiative capture processes [3–6]. In the R -matrix approach the ANC determines the normalization of the external nonresonant radiative capture amplitude and the channel radiative reduced width amplitude [7–9]. In Refs. [10,11] relationships between mirror proton and neutron ANCs were obtained.

Pairs of nuclei B_1 and B_2 are mirror nuclei if the number of protons Z_1 of nucleus B_1 equals the number of neutrons N_2 of B_2 and the number of protons of B_2 , Z_2 , equals the number of neutrons N_1 of B_1 , such that the mass number of both nuclei is the same ($A = N_1 + Z_1 = N_2 + Z_2$). The experimental data from mirror nuclei show charge symmetry of the nuclear force. It is assumed that charge symmetry rather than full charge independence is involved because mirror nuclei have the same number of p - n pairs.

However, the ANCs are important characteristics not only of the bound states but also of the resonances (see Ref. [9]). The width of a narrow resonance can be expressed in terms of the ANC of the Gamow wave function or of the R -matrix resonant outgoing wave. That is why the relationship between the ANCs of mirror bound states [10,11] can be extended to the relationship between resonance widths and ANCs of the mirror nuclei. The calculated resonance widths and the ANCs

themselves depend strongly on the choice of the nucleon-nucleon (NN) force but the ratios of the resonance widths and the ANCs for mirror pairs should not depend on the choice of the NN force. This observation is based thus far entirely on the calculations using detailed models of nuclear structure. It follows naturally as a consequence of the charge symmetry of nuclear forces. Mirror nuclei have the same quantum numbers of mirror states (for more detailed discussion of mirror symmetry see Ref. [12]).

Another important feature of the mirror nuclei for the present paper is a similarity of the internal mirror wave functions. Let us consider a mirror pair in a two-body potential model, which is used in the present paper: $B_1 = (a_1A_1)$ in the resonance state and the loosely bound nucleus $B_2 = (a_2A_2)$. The mirror resonance state is obtained by the replacement of one of the neutrons by a proton. The additional Coulomb interaction pushes the bound-state level into a resonance level. The resonance and binding energy of the mirror states are significantly smaller than the depth of the nuclear potential. The Coulomb interaction is almost a constant in the nuclear interior. Hence, in the nuclear interior, where all that matters is to determine the ratio of the resonance width and the ANC of the mirror state, the radial behavior of the mirror wave functions is very similar and they differ only by normalization. In the external region the resonant and bound-state wave functions differ.

The first attempt to relate the resonance width and the ANC of the mirror nuclei was done in Ref. [10]. In this paper, the relationship between the resonance widths and the ANCs is established based on the Pinkston-Satchler equation used

in Ref. [11] for the ANC of the mirror bound states. The obtained ratio of the resonance width and the ANC of the mirror bound state is expressed in terms of the ratio of the Wronskians containing the overlap functions of the mirror resonance and bound states in the internal region where the radial behavior of the mirror overlap functions is very similar and can be calculated quite accurately using an *ab initio* approach. If these overlap functions are not available, as an approximation they can be replaced by the mirror resonance and bound-state wave functions calculated using the two-body potential model with the same potentials for the resonance and bound states. Assuming that the radial behavior of the mirror resonant and bound-state wave functions is identical in the nuclear interior one can replace the Wronskian ratio for the resonance width and the ANC of the mirror bound state by the equation derived in Ref. [10], which does not require a knowledge of the internal resonant and bound-state wave functions.

Connection between the ANC and the resonance width of the mirror resonance state provides a powerful indirect method to obtain information which is unavailable directly. If, for instance, the resonance width is unknown it can be determined through the known ANC of the mirror state and vice versa. For example, near the edge of the stability valley, neutron binding energies become so small that the mirror proton states are resonances. Using the relationship between the mirror resonance width and the ANC the resonance width can be determined. Also loosely bound states $\alpha + A$ become resonances in the mirror nucleus $\alpha + B$, where charge $Z_B e > Z_A e$. Using the method developed here one can find one of the missing quantities, the resonance width of the narrow resonance state or the mirror ANC. In what follows the system of units in which $\hbar = c = 1$ is used throughout the paper.

II. ANC AND RESONANCE WIDTH

A. ANC as residue of S matrix

The ANC enters the theory in two ways [1]. In the scattering theory the residue at the poles of the elastic scattering S matrix corresponding to bound states can be expressed in terms of the ANC:

$$S_{l_B j_B; l_B j_B}^{j_B} \xrightarrow{k_{aA} \rightarrow k_{aA}^{bs}} \frac{A_{l_B j_B}}{k - i\kappa_{aA}} \quad (1)$$

with the residue

$$A_{l_B j_B}^{j_B} = -i^{2l_B+1} e^{i\pi \eta_{aA}^{bs}} (C_{aA l_B j_B}^B)^2. \quad (2)$$

Here, $C_{aA l_B j_B}^B$ is the ANC for the virtual decay of the bound state $B(aA)$ in the channel with the relative orbital angular momentum l_B of a and A , the total angular momentum j_B of a , and total angular momentum J_B of the system $a + A$; k_{aA} is the relative momentum of particles a and A . Here

$$\eta_{aA}^{bs} = \frac{Z_a Z_A e^2 \mu_{aA}}{\kappa_{aA}} \quad (3)$$

is the Coulomb parameter for the bound state $B = (aA)$, $\kappa_{aA} = \sqrt{2\mu_{aA} \varepsilon_{aA}}$ is the bound-state wave number, $\varepsilon_B = m_a + m_A - m_B$ is the binding energy for the virtual decay $B \rightarrow a + A$, $Z_i e$ and m_i are the charge and mass of particle i , and

μ_{aA} is the reduced mass of a and A . Note that singling out the factor $e^{i\pi \eta_{aA}^{bs}}$ in the residue makes the ANC for bound states real.

Equations (1) and (2), which were proved for the bound states in Refs. [13–18], can be extended for resonance states.

B. Connection between ANC and resonance width

The proof of the connection between the residue in the resonance pole of the elastic scattering S matrix and the ANC of the resonance state is not trivial. In this section a general proof is presented of the connection of the residue in the pole of the $S_{l_B}(k_{aA})$ matrix element with the ANC, which is valid for both the bound states and resonances. The potential is given by the sum of the short-range nuclear plus the long-range Coulomb potentials. Taking into account that the residue of the elastic scattering S matrix in the resonance pole is expressed in terms of the resonance width, one can obtain a connection between the ANC and the resonance width.

One considers two spinless particles a and A with relative momentum $k_{aA}^2 = 2\mu_{aA} E_{aA}$, relative energy E_{aA} , and the reduced mass μ_{aA} in the partial wave l_B at which the system $B = a + A$ has a resonance or a bound state. The radial wave function $\psi_{k_{aA} l_B}(r) = \frac{u_{k_{aA} l_B}(r)}{r}$ satisfies the Schrödinger equation in the partial wave l_B :

$$\frac{\partial^2 u_{k_{aA} l_B}(r)}{\partial r^2} + \left[k_{aA}^2 - 2\mu_{aA} V(r) - \frac{l_B(l_B + 1)}{r^2} \right] u_{k_{aA} l_B}(r) = 0. \quad (4)$$

Here $V(r) = V^N(r) + V^C(r)$, $V^N(r)$ is the short-range nuclear potential, and $V^C(r)$ is the long-range Coulomb one. For potentials satisfying the condition $\lim_{r \rightarrow 0} r^2 V(r) \rightarrow 0$,

$$u_{k_{aA} l_B}(r) \sim r^{l_B+1}, \quad r \rightarrow 0. \quad (5)$$

Now one should take the derivative over k_{aA} from the left-hand side of Eq. (4), multiply the result by $u_{k_{aA} l_B}(r)$, and subtract from it Eq. (4) multiplied by $\partial u_{k_{aA} l_B}(r)/\partial k_{aA}$. Integrating the obtained expression from $r = 0$ until $r = R$ and taking into account Eq. (5) one gets

$$\int_0^R dr u_{k_{aA} l_B}^2(r) = \frac{1}{2k_{aA}} \left[\frac{\partial u_{k_{aA} l_B}(R)}{\partial k_{aA}} \frac{\partial u_{k_{aA} l_B}(R)}{\partial R} - u_{k_{aA} l_B}(R) \frac{\partial^2 u_{k_{aA} l_B}(R)}{\partial k_{aA} \partial R} \right]. \quad (6)$$

Taking R so large that $u_{k_{aA} l_B}(R)$ can be replaced by its leading asymptotic term, one gets the elastic scattering wave function

$$u_{k_{aA} l_B}(R) \approx \tilde{C}_{l_B} [e^{i\rho} - (-1)^{l_B} S_{l_B}^{-1}(k_{aA}) e^{-i\rho}], \quad (7)$$

where $\rho = k_{aA} R - \eta_{aA} \ln 2k_{aA} R$, $\eta_{aA} = \frac{Z_a Z_A e^2 \mu_{aA}}{k_{aA}}$ is the Coulomb parameter of the $a + A$ system,

$$S_{l_B}(k_{aA}) = e^{2i[\sigma_{l_B}^C(k_{aA}) + \delta_{l_B}^{CN}(k_{aA})]} \quad (8)$$

is the elastic scattering S -matrix element, $\sigma_{l_B}^C(k_{aA})$ and $\delta_{l_B}^{CN}(k_{aA})$ are the Coulomb and Coulomb-modified nuclear scattering phase shifts in the l_B th partial wave, and \tilde{C}_{l_B} is a

constant, which is in the pole of the S -matrix and is related to the corresponding ANC C_{l_B} [see Eqs. (14) and (15) below]. Note that the scattering wave function $u_{k_{aA}l_B}$ at large R at real momentum k_{aA} contains ingoing and outgoing waves and is not normalizable in the entire space.

Assume that the elastic scattering $S_{l_B}(k_{aA})$ -matrix element has a first order pole at $k_{aA} = k_p$ with the residue A_{l_B} corresponding to the bound state $k_p = i\kappa_{aA}$ or to the resonance $k_p = k_{aA(\mathcal{R})} = k_{aA(0)} - \text{Im}k_{aA(\mathcal{R})}$, where $k_{aA(0)} = \text{Re}k_{aA(\mathcal{R})}$:

$$S_{l_B}(k_{aA}) = \frac{A_{l_B}}{k_{aA} - k_p} + g_{l_B}(k_{aA}), \quad (9)$$

where $g_{l_B}(k_{aA})$ is a regular function at $k_{aA} = k_p$.

Substituting Eqs. (7) and (9) into the right-hand side of Eq. (6) and performing the differentiation over k_{aA} and R and taking $k_{aA} = k_p$ one gets

$$\int_0^R dr u_{k_p l_B}^2(r) = i(-1)^{l_B+1} \tilde{C}_{l_B}^2 / A_{l_B} - \frac{i}{2k_p} e^{2i\rho_p}. \quad (10)$$

Here $\rho_p = k_p R - \eta_p \ln(2k_p R)$. On the left-hand side under the integral sign one has the function $u_{k_p l_B}^2(r)$, which is regular at $r = 0$ [see Eq. (5)].

Note that at the pole $k_{aA} = k_p$, $S_{l_B}^{-1}(k_p) = 0$, and one can see from Eq. (7) that in the external region the wave function $u_{k_p l_B}(R)$ satisfies the radiation condition

$$u_{k_p l_B}(r) \stackrel{r \rightarrow \infty}{\approx} \tilde{C}_{l_B} e^{i\rho_p}. \quad (11)$$

For the bound state $k_p = i\kappa_{aA}$ and

$$u_{i\kappa_{aA} l_B}(r) \stackrel{r > R_N}{\approx} C_{l_B} W_{-\eta_{aA}^{bs}, l_B+1/2}(2\kappa_p r) \approx C_{l_B} e^{-\kappa_{aA} r - \eta_{aA}^{bs} \ln(2\kappa_{aA} r)}, \quad (12)$$

where R_N is the $a-A$ nuclear interaction radius. For the resonance state $k_p = k_{aA(\mathcal{R})}$ and $u_{k_{aA(\mathcal{R})} l_B}(r)$ is the resonance Gamow wave function with the resonance energy $E_{aA(\mathcal{R})}$:

$$u_{k_{aA(\mathcal{R})} l_B}(r) \stackrel{r > R_N}{\approx} C_{l_B} W_{-i\eta_{aA}^{(R)}, l_B+1/2}(-2ik_{aA(\mathcal{R})} r) \approx e^{-\pi\eta_{aA}^{(R)}/2} C_{l_B} e^{ik_{aA(\mathcal{R})} r - i\eta_{aA}^{(R)} \ln(2k_{aA(\mathcal{R})} r)} = \tilde{C}_{l_B} e^{ik_{aA(\mathcal{R})} r - i\eta_{aA}^{(R)} \ln(2k_{aA(\mathcal{R})} r)}. \quad (13)$$

Here, $\eta_{aA}^{(R)} = \frac{Z_a Z_A e^2 \mu_{aA}}{k_{aA(\mathcal{R})}}$ is the $a+A$ Coulomb parameter of the resonance.

The constant \tilde{C}_{l_B} is related to the ANC C_{l_B} as $\tilde{C}_{l_B} = e^{-\pi\eta_p/2} C_{l_B}$, where $\eta_p = \frac{Z_a Z_A e^2 \mu_{aA}}{k_p}$. For the resonances one has

$$\tilde{C}_{l_B} = e^{-\pi\eta_{aA}^{(R)}/2} C_{l_B} \quad (14)$$

and for the bound states

$$\tilde{C}_{l_B} = e^{i\pi\eta_{aA}^{bs}/2} C_{l_B}. \quad (15)$$

Note that C_{l_B} , which is real for the bound states, is the standard definition of the ANC for the bound states and is used in this paper for the bound states.

For the bound states the asymptotic of the bound-state wave function is exponentially decaying and the bound-state wave function can be normalized. The Gamow wave

function of the resonance state asymptotically oscillates and is exponentially increasing. To normalize the Gamow wave function one can use the Zel'dovich regularization procedure [17], which is a particular case of the more general Abel regularization:

$$\lim_{\beta \rightarrow +0} \int_0^\infty dr e^{-\beta r^2} u_{k_{aA(\mathcal{R})} l_B}^2(r) = 1. \quad (16)$$

For the bound state one can take under the integral sign $\beta = 0$ and obtain the usual normalization procedure. For the resonance state one can take the limit $\beta \rightarrow 0$ only after performing the integration over r . Note that Zel'dovich normalization was introduced for exponentially decaying potentials. In the Appendix it is shown that the Zel'dovich regularization procedure works even for the Coulomb potentials.

For any finite R one can rewrite Eq. (16) as

$$\int_0^R dr u_{k_{aA(\mathcal{R})} l_B}^2(r) + \lim_{\beta \rightarrow +0} \int_R^\infty dr e^{-\beta r^2} u_{k_{aA(\mathcal{R})} l_B}^2(r) = 1. \quad (17)$$

Assume that R is so large that one can use the asymptotic expression (11) and Eq. (A6) of the Appendix. It leads to

$$\int_0^R dr u_{k_{aA(\mathcal{R})} l_B}^2(r) = 1 - \frac{i}{2k_{aA(\mathcal{R})}} \tilde{C}_{l_B}^2 e^{2i\rho_p}. \quad (18)$$

Comparing Eqs. (10) and (18) one arrives at the final equation, which expresses the residue in the pole of the elastic scattering S -matrix in terms of the ANC:

$$A_{l_B} = -i^2 l_B + 1 \tilde{C}_{l_B}^2. \quad (19)$$

Equation (19) is universal and valid for bound-state poles and resonances. In terms of the standard ANC C_{l_B} the residue in the resonance pole is

$$A_{l_B} = -i^2 l_B + 1 e^{-\pi\eta_{aA}^{(R)}} C_{l_B}^2 \quad (20)$$

and for the bound state it is given by Eq. (2).

Now it is shown how to relate the ANC \tilde{C}_{l_B} to the resonance width Γ_{aA} . Here the following definitions are used:

$$E_{aA(\mathcal{R})} = k_{aA(\mathcal{R})}^2 / (2\mu_{aA}) = E_{aA(0)} - i\Gamma_{aA} / 2, \\ E_{aA(0)} = [k_{aA(0)}^2 - (\text{Im}k_{aA(\mathcal{R})})^2] / (2\mu_{aA}), \\ \Gamma_{aA} = 2k_{aA(0)} \text{Im}k_{aA(\mathcal{R})} / \mu_{aA}. \quad (21)$$

One can write

$$S_{l_B}(k_{aA}) = e^{2i\delta_{l_B}^{\text{pot}}} \frac{(k_{aA} + k_p)(k_{aA} - k_p^*)}{(k_{aA} - k_p)(k_{aA} + k_p^*)}, \quad (22)$$

where $\delta_{l_B}^{\text{pot}}$ is the nonresonant scattering phase shift. At $k_p = k_{aA(\mathcal{R})}$ and at $k_{aA} \rightarrow k_{aA(\mathcal{R})}$

$$A_{l_B}(k_{aA}) = -2ik_{aA(\mathcal{R})} \gamma [(1 + \gamma^2)^{1/4} + (1 + \gamma^2)^{-1/4}]^{-1} \times e^{i[2\delta_{l_B}^{\text{pot}}(k_{aA(\mathcal{R})}) - 1/2 \arctan(\gamma)]}, \quad (23)$$

$\gamma = \frac{\Gamma_{aA}}{2E_{aA(0)}}$. Equation (23) expresses the residue of the S -matrix elastic scattering element in terms of the resonance energy and the resonance width for broad resonances.

236 Recovering now all the quantum numbers one gets for a
237 narrow resonance ($\gamma \ll 1$) up to terms of order $\sim \gamma$

$$(\tilde{C}_{aA l_B j_B J_B}^B)^2 = i^{-2l_B} e^{i2\delta_{l_B j_B J_B}^p(k_{aA(0)})} \frac{\mu_{aA} \Gamma_{aA l_B j_B J_B}}{k_{aA(0)}}, \quad (24)$$

238 where $\Gamma_{aA l_B j_B J_B}$ is the resonance width and $\delta_{l_B j_B J_B}^p(k_{aA}^0)$ is the
239 potential (nonresonance) scattering phase shift at the real res-
240 onance relative momentum $k_{aA(0)}$. This equation is the desired
241 equation, which relates the ANC of the narrow resonance to
242 the resonance width.

243 The residue in the resonance pole with all the quantum
244 numbers recovered is

$$A_{l_B j_B}^{J_B} = -i^{2l_B+1} (\tilde{C}_{aA l_B j_B J_B}^B)^2. \quad (25)$$

245 For the Breit-Wigner resonance ($\text{Im}k_{aA(\mathcal{R})} \ll \text{Re}k_{aA(\mathcal{R})} =$
246 $k_{aA(0)}$), Eq. (25) takes the form

$$A_{l_B j_B}^{J_B} = -i^{2l_B+1} e^{-\pi \eta_{aA(0)}} (\tilde{C}_{aA l_B j_B J_B}^B)^2 = -i^{2l_B+1} (\tilde{C}_{aA l_B j_B J_B}^B)^2, \quad (26)$$

247 where $\eta_{aA(0)} = Z_a Z_A e^2 \mu_{aA}/k_{aA(0)}$. In terms of the resonance
248 width the residue of the elastic scattering S -matrix element in
249 the resonance pole is

$$A_{l_B j_B}^{J_B} = -i e^{2i\delta_{l_B j_B J_B}^p(k_{aA}^0)} \frac{\mu_{aA}}{k_{aA(0)}} \Gamma_{aA l_B j_B J_B}. \quad (27)$$

250 III. ANCS AND OVERLAP FUNCTIONS

251 Equations obtained in the previous section, which express
252 the residues of the S -matrix elastic element in terms of the
253 ANCs of the bound states and resonances, provide the most
254 general and model-independent definition of the ANCs. From
255 other side, in the Schrödinger formalism of the wave functions
256 the ANC is defined as the amplitude of the tail of the overlap
257 function of the bound-state wave functions of B , A , and a . The
258 overlap function is given by

$$\begin{aligned} I_{aA}(\mathbf{r}_{aA}) &= \langle \psi_c | \varphi_B(\xi_A, \xi_a, \mathbf{r}_{aA}) \rangle \\ &= \sum_{l_B m_{l_B} j_B m_{j_B}} \langle J_A M_A j_B m_{j_B} | J_B M_B \rangle \langle J_a M_a l_B m_{l_B} | j_B m_{j_B} \rangle \\ &\quad \times Y_{l_B m_{l_B}}(\hat{\mathbf{r}}_{aA}) I_{aA l_B j_B J_B}(r_{aA}). \end{aligned} \quad (28)$$

259 Here

$$\begin{aligned} \psi_c &= \sum_{m_{j_B} m_{l_B} M_A M_a} \langle J_A M_A j_B m_{j_B} | J_B M_B \rangle \langle J_a M_a l_B m_{l_B} | j_B m_{j_B} \rangle \\ &\quad \times \hat{A}_{aA} \{ \varphi_A(\xi_A) \varphi_a(\xi_a) Y_{l_B m_{l_B}}(\hat{\mathbf{r}}_{aA}) \} \end{aligned} \quad (29)$$

260 is the two-body $a + A$ channel wave function in the jj
261 coupling scheme, $\langle j_1 m_1 j_2 m_2 | j m \rangle$ is the Clebsch-Gordan
262 coefficient, \hat{A}_{aA} is the antisymmetrization operator between
263 the nucleons of nuclei a and A , $\varphi_i(\xi_i)$ represents the fully
264 antisymmetrized bound-state wave function of nucleus i with
265 ξ_i being a set of the internal coordinates including spin-isospin
266 variables, and J_i and M_i are the spin and its projection of
267 nucleus i . Also \mathbf{r}_{aA} is the radius vector connecting the centers
268 of mass of nuclei a and A , $\hat{\mathbf{r}}_{aA} = \mathbf{r}_{aA}/r_{aA}$, $Y_{l_B m_{l_B}}(\hat{\mathbf{r}}_{aA})$ is the
269 spherical harmonics, and $I_{aA l_B j_B J_B}(r_{aA})$ is the radial overlap
270 function. Notations of the spins and angular momenta are

271 given in Sec. II A. The summation over l_B and j_B is carried
272 out over the values allowed by the angular momentum and
273 parity conservation in the virtual process $B \rightarrow A + a$.

The radial overlap function is given by

$$\begin{aligned} I_{aA l_B j_B J_B}(r_{aA}) &= \langle \hat{A}_{aA} \{ \varphi_A(\xi_A) \varphi_a(\xi_a) Y_{l_B m_{l_B}}(\hat{\mathbf{r}}_{aA}) \} | \varphi_B(\xi_A, \xi_a; \mathbf{r}_{aA}) \rangle \\ &= \left(\frac{A}{a} \right)^{\frac{1}{2}} \langle \varphi_A(\xi_A) \varphi_a(\xi_a) Y_{l_B m_{l_B}}(\hat{\mathbf{r}}_{aA}) | \varphi_B(\xi_A, \xi_a; \mathbf{r}_{aA}) \rangle. \end{aligned} \quad (30)$$

275 Equation (30) follows from a trivial observation that, because
276 φ_B is fully antisymmetrized, the antisymmetrization operator
277 \hat{A}_{aA} can be replaced by the factor $(\frac{A}{a})^{\frac{1}{2}}$. In what follows, in
278 contrast to Blokhintsev *et al.* [1], I absorb this factor into the
279 radial overlap function.

280 The tail of the radial overlap function ($r_{aA} > R_{aA}$) in the
281 case of the normal asymptotic behavior is given by

$$\begin{aligned} I_{aA l_B j_B J_B}(r_{aA}) &= C_{aA l_B j_B J_B}^B \frac{W_{-\eta_{aA}, l_B+1/2}(2\kappa_{aA} r_{aA})}{r_{aA}} \\ &\xrightarrow{r_{aA} \rightarrow \infty} C_{aA l_B j_B J_B}^B \frac{e^{-\kappa_{aA} r_{aA} - \eta_{aA}^{\text{bs}} \ln(2\kappa_{aA} r_{aA})}}{r_{aA}}. \end{aligned} \quad (31)$$

282 Formally the radial resonance overlap function for the
283 Breit-Wigner resonance in the external region ($r_{aA} > R_{aA}$) can
284 be obtained from Eq. (31) by the substitution $\kappa_{aA} = -i k_{aA(\mathcal{R})}$:

$$\begin{aligned} I_{aA l_B j_B J_B}(k_{aA(\mathcal{R})}, r_{aA}) &= C_{aA l_B j_B J_B}^B \frac{W_{-i\eta_{aA}^{(\mathcal{R})}, l_B+1/2}(-2i k_{aA(\mathcal{R})} r_{aA})}{r_{aA}} \\ &\xrightarrow{r_{aA} \rightarrow \infty} C_{aA l_B j_B J_B}^B \frac{e^{i k_{aA(\mathcal{R})} r_{aA} - i \eta_{aA}^{(\mathcal{R})} \ln(-2i k_{aA(\mathcal{R})} r_{aA})}}{r_{aA}} \\ &= \tilde{C}_{aA l_B j_B J_B}^B \frac{e^{i k_{aA(\mathcal{R})} r_{aA} - i \eta_{aA}^{(\mathcal{R})} \ln(2 k_{aA(\mathcal{R})} r_{aA})}}{r_{aA}}. \end{aligned} \quad (32)$$

285 This asymptotic behavior agrees with the asymptotic behavior
286 of the resonant Gamow wave function given by Eq. (13).

287 IV. R-MATRIX WAVE FUNCTIONS

288 Because the microscopic overlap functions for mirror res-
289 onances and bound states are not available, in this paper I use
290 internal resonance and bound-state wave functions calculated
291 in the the potential model. If the mirror symmetry holds,
292 the bound-state and resonance wave functions of the mirror
293 states should be very similar in the internal region where the
294 resonance wave functions are real. However, both wave func-
295 tions differ in the external region where the bound-state wave
296 functions exponentially decrease while the resonance wave
297 functions at the resonance energies exponentially increase
298 (see Sec. III). In the Wronskian method, which is developed
299 in this paper, one needs the wave functions in the internal
300 region in which it is very convenient to use the R -matrix
301 method. In the R -matrix method the resonant wave functions
302 are normalized to unity in the internal region. The border
303 of this region is determined by the point at which the radial

304 derivative of the internal resonant wave function is equal to
 305 zero. If the resonant wave function has a few nodes, the border
 306 of the internal region is determined by the last point at which
 307 the radial derivative of the resonant wave function vanishes.
 308 To make the bound-state wave functions close to the resonant
 309 wave functions the former are also renormalized to unity in
 310 the internal region.

311 In the R -matrix approach the resonant wave function is
 312 considered at the real part of the resonance energy $E_{aA(0)}$. In
 313 this approach the internal wave function at real energies is real
 314 and behaves similarly to the bound-state wave function of the
 315 mirror state. At the R -matrix channel radius R_{ch} and $E_{aA} =$
 316 $E_{aA(0)}$ the internal wave function coincides with the external
 317 one and is proportional to the outgoing wave $O_{l_B}(k_{aA(0)}, R_{\text{ch}})$.
 318 Below I present the internal and external R -matrix wave
 319 functions considering the single-level, single-channel case.
 320 Again, for simplicity, the particles are assumed to be spinless.

321 I start from the external R -matrix wave function at the
 322 partial wave l_B , which is given by [11,19]

$$X_{l_B}^{(\text{ext})(+)}(\mathbf{k}_{aA}, \mathbf{r}_{aA}) = i^{l_B+1} \frac{2\pi}{k_{aA} r_{aA}} Y_{l_B m_{l_B}}^*(\hat{\mathbf{k}}_{aA}) Y_{l_B m_{l_B}}(\hat{\mathbf{r}}_{aA}) \times [I_B - S_{l_B} O_{l_B}(k_{aA}, r_{aA})], \quad (34)$$

323 where

$$S_{l_B} = e^{-2i[\delta_{l_B}^{\text{hs}} - \sigma_{l_B}^C]} \left(1 + \frac{i\Gamma_{l_B}}{E_R - E_{aA} - \frac{i\Gamma_{l_B}}{2}} \right) \quad (35)$$

324 is the elastic scattering S matrix at E_{aA} near the real resonance
 325 energy $E_{aA(0)}$. $\sigma_{l_B}^C$ is the Coulomb scattering phase shift and
 326 $\delta_{l_B}^{\text{hs}}$ is the R -matrix hard-sphere scattering phase shift:

$$e^{-2i\delta_{l_B}^{\text{hs}}} = \frac{G_{l_B}(k_{aA}, R_{\text{ch}}) - iF_{l_B}(k_{aA}, R_{\text{ch}})}{G_{l_B}(k_{aA}, R_{\text{ch}}) + iF_{l_B}(k_{aA}, R_{\text{ch}})}, \quad (36)$$

327 $F_{l_B}(k_{aA}, r_{aA})$ and $G_{l_B}(k_{aA}, r_{aA})$ are the regular and singular
 328 Coulomb solutions, and R_{ch} is the R -matrix channel radius.

329 The outgoing wave is given by

$$O_{l_B}(k_{aA}, r_{aA}) = (G_{l_B}(k_{aA}, r_{aA}) + iF_{l_B}(k_{aA}, r_{aA})) e^{-i\sigma_{l_B}^C}. \quad (37)$$

330 At $r_a = R_{\text{ch}}$

$$O_{l_B}(k_{aA}, R_{\text{ch}}) = e^{i[\delta_{l_B}^{\text{hs}} - \sigma_{l_B}^C]} \sqrt{F_{l_B}^2(k_{aA}, R_{\text{ch}}) + G_{l_B}^2(k_{aA}, R_{\text{ch}})}. \quad (38)$$

331 $O_{l_B}(k_{aA}, r_{aA})$ can be expressed it terms of the Whittaker
 332 function:

$$O_{l_B}(k_{aA}, r_{aA}) = i^{-l_B} e^{\pi \eta_{aA}/2} W_{-i\eta_{aA}, l_B+1/2}(-2i k_{aA} r_{aA}). \quad (39)$$

At $r_{aA} = R_{\text{ch}}$ and $E_{aA} = E_{aA(0)}$

333

$$X_{l_B}^{(\text{ext})(+)}(\mathbf{k}_{aA(0)}, \mathbf{R}_{\text{ch}}) = i^{l_B+1} \frac{4\pi}{k_{aA(0)} R_{\text{ch}}} e^{-2i[\delta_{l_B}^{\text{hs}} - \sigma_{l_B}^C]} Y_{l_B m_{l_B}}^* \times (\hat{\mathbf{k}}_{aA(0)}) Y_{l_B m_{l_B}}(\hat{\mathbf{R}}_{\text{ch}}) O_{l_B}(k_{aA(0)}, R_{\text{ch}}). \quad (40)$$

The R -matrix internal resonant wave function in the partial
 wave l_B , in which the resonant is present, at energy E_{aA} near
 the resonance is given by

334

335

336

$$X_{l_B}^{(\text{int})(+)}(\mathbf{k}_{aA}, \mathbf{r}_{aA}) = i^{l_B} \frac{2\pi}{k_{aA} r_{aA}} \sqrt{\frac{k_{aA}}{\mu_{aA}}} e^{-i[\delta_{l_B}^{\text{hs}} - \sigma_{l_B}^C]} Y_{l_B m_{l_B}}^*(\hat{\mathbf{k}}_{aA}) \times Y_{l_B m_{l_B}}(\hat{\mathbf{r}}_{aA}) \frac{\Gamma_{l_B}^{1/2}}{E_R - E_{aA} - i\frac{\Gamma_{l_B}}{2}} \times \phi_{l_B}^{(\text{int})}(k_{aA}, r_{aA}). \quad (41)$$

The R -matrix internal resonant wave function
 $\phi_{l_B}^{(\text{int})}(k_{aA}, r_{aA})$ can be found as a solution of the Schrödinger
 equation with the two-body Woods-Saxon V_{aA} potential.
 The R -matrix method is used below for mirror resonance
 and bound states. I consider the loosely bound states which
 become the mirror resonances by replacing one of the
 neutrons by a proton. The considered binding energies
 and real energies of the mirror resonances are significantly
 smaller than the depth of the potential. That is why both
 mirror solutions of the Schrödinger equation should be very
 similar in the internal region where both solutions are real.

337

338

339

340

341

342

343

344

345

346

347

At $r_{aA} = R_{\text{ch}}$ and $E_{aA} = E_{aA(0)}$ [see Eq. A(10); from
 Ref. [11] in which the reduced width amplitude should be
 expressed in terms of the resonance width] it follows that

348

349

350

$$\phi_{l_B}^{(\text{int})}(k_{aA(0)}, R_{\text{ch}}) = \sqrt{\frac{\mu_{aA} \Gamma_{l_B}}{k_{aA(0)}}} e^{-i[\delta_{l_B}^{\text{hs}} - \sigma_{l_B}^C]} O_{l_B}(k_{aA(0)}, R_{\text{ch}}). \quad (42)$$

Thus at the real part of the resonance energy $E_{aA} = E_{aA(0)}$
 and $r_{aA} = R_{\text{ch}}$ the internal radial wave function $\phi_{l_B}^{(\text{int})}(R_{\text{ch}})$ is
 proportional to the outgoing wave $O_{l_B}(k_{aA(0)}, R_{\text{ch}})$. Equation
 (42) also follows from the matching of the internal and
 external wave radial wave function (see below).

351

352

353

354

355

Taking into account Eq. (24) and that in the R -matrix
 approach the potential scattering phase shift is $\delta_{l_B} = -(\delta_{l_B}^{\text{hs}} -$
 $\sigma_{l_B}^C)$ one gets

356

357

358

$$\phi_{l_B}^{(\text{int})}(k_{aA(0)}, R_{\text{ch}}) = C_{l_B} W_{-i\eta_{aA(0)}, l_B+1/2}(-2i k_{aA(0)} R_{\text{ch}}), \quad (43)$$

$$\eta_{aA(0)} = \frac{Z_a Z_A e^2 \mu_{aA}}{k_{aA(0)}}.$$

359

At $r_{aA} = R_{\text{ch}}$ and $E_{aA} = E_{aA(0)}$ one gets

360

$$X_{l_B}^{(\text{int})(+)}(\mathbf{k}_{aA(0)}, \mathbf{R}_{\text{ch}}) = i^{l_B+1} \frac{4\pi}{k_{aA} r_{aA}} e^{-2i[\delta_{l_B}^{\text{hs}} - \sigma_{l_B}^C]} \times Y_{l_B m_{l_B}}^*(\hat{\mathbf{k}}_{aA}) Y_{l_B m_{l_B}}(\hat{\mathbf{R}}_{\text{ch}}) \times O_{l_B}(k_{aA(0)}, R_{\text{ch}}). \quad (44)$$

361 Thus at $r_{aA} = R_{ch}$ and $E_{aA} = E_{aA(0)}$ one gets matching of
 362 the internal and external R -matrix wave functions,

$$X_{l_B}^{(ext)(+)}(\mathbf{k}_{aA(0)}, \mathbf{R}_{ch}) = X^{(int)(+)}(\mathbf{k}_{aA(0)}, \mathbf{R}_{ch}), \quad (45)$$

363 and both wave functions are proportional to the outgoing wave
 364 $O_{l_B}(k_{aA}, R_{ch})$.

365 One can write the radial overlap function
 366 $I_{aA l_B j_B J_B}(k_{aA(0)}, R_{ch})$ in terms of the outgoing wave
 367 $O_{l_B}(k_{aA(0)}, R_{ch})$ and the Whittaker function:

$$\begin{aligned} I_{aA l_B j_B J_B}(k_{aA(0)}, R_{ch}) &= \tilde{C}_{aA l_B j_B J_B}^B i^{l_B} \frac{O_{l_B}(k_{aA(0)}, R_{ch})}{R_{ch}} \\ &= \sqrt{\frac{\mu_{aA}}{k_{aA(0)}}} \Gamma_{aA l_B j_B J_B} e^{-i[\delta_{l_B}^{hs} - \sigma_{l_B}^C]} \frac{O_{l_B}(k_{aA(0)}, R_{ch})}{R_{ch}} \\ &= C_{aA l_B j_B J_B}^B \frac{W_{-i\eta_{aA(0)}, l_B + 1/2}(k_{aA(0)}, R_{ch})}{R_{ch}} \\ &= i^{-l_B} e^{-i[\delta_{l_B}^{hs} - \sigma_{l_B}^C]} e^{\pi \eta_{aA(0)}/2} \sqrt{\frac{\mu_{aA}}{k_{aA(0)}}} \Gamma_{aA l_B j_B J_B} \\ &\quad \times \frac{W_{-i\eta_{aA(0)}, l_B + 1/2}(k_{aA(0)}, R_{ch})}{R_{ch}}. \end{aligned} \quad (46)$$

368 As one can see, the resonant radial overlap function calcu-
 369 lated in the R -matrix at the channel radius $r_{aA} = R_{ch}$ and
 370 $E_{aA} = E_{aA(0)}$ is proportional to the the square root of the
 371 resonance width. It is convenient to use the R -matrix method
 372 to determine the ratio of the resonance width and the bound-
 373 state ANC of the mirror states using the Wronskian method
 374 developed below.

375 **V. CONNECTION BETWEEN BREIT-WIGNER**
 376 **RESONANCE WIDTH AND ANC OF MIRROR**
 377 **RESONANCE AND BOUND STATES FROM**
 378 **PINKSTON-SATCHLER EQUATION**

379 **A. ANC and Pinkston-Satchler equation**

380 In Ref. [11] the relationship between the mirror proton
 381 and neutron ANCs was derived using the Pinkston-Satchler
 382 equation [20,21]. Here I extend this derivation to obtain the

383 ratio for the resonance width and the ANC of the mirror bound
 384 state in terms of the Wronskians, which follows from the
 385 Pinkston-Satchler equation.

386 First, using Pinkston-Satchler equation I derive the equa-
 387 tion for the ANC of the narrow resonance state, which con-
 388 tains the source term [6,22]. This derivation is valid for both
 389 bound and resonance states. That is why following [11] I start
 390 from the Schrödinger equation for the resonance scattering
 391 wave function at the real part $E_{aA(0)}$ of the resonance energy:

$$(E_{(0)} - \hat{T}_A - \hat{T}_a - \hat{T}_{aA} - V_a - V_A - V_{aA})\Psi(\xi_A, \xi_a; \mathbf{r}_{aA}) = 0. \quad (47)$$

392 Here, \hat{T}_i is the internal motion kinetic energy operator of
 393 nucleus i , \hat{T}_{aA} is the kinetic energy operator of the relative
 394 motion of nuclei a and A , V_i is the internal potential of nucleus
 395 i and V_{aA} is the interaction potential between a and A , and
 396 $E_{(0)} = E_{aA(0)} - \varepsilon_a - \varepsilon_A$ is the total energy of the system $a + A$
 397 in the continuum. The operator $E_{(0)} - \hat{T}_A - \hat{T}_a - \hat{T}_{aA} - V_a -$
 398 $V_A - V_{aA}$ in Eq. (47) is symmetric over the interchange of
 399 nucleons of a and A , while $\Psi(\xi_a, \xi_A; \mathbf{r}_{aA})$ is antisymmetric,
 400 and ε_i is the total binding energy of nucleus i . Hence, by
 401 multiplying the Schrödinger equation (47) from the left by

$$\begin{aligned} \left(\begin{matrix} A \\ a \end{matrix}\right)^{1/2} \sum_{m_j m_B M_A M_a} \langle J_A M_A j_B m_j | J_B M_B \rangle \\ \times \langle J_a M_a l_B m_l | j_B m_j \rangle Y_{l_B m_l}^*(\hat{\mathbf{r}}_{aA}) \varphi_A(\xi_A) \varphi_a(\xi_a), \end{aligned} \quad (48)$$

402 where the antisymmetrization operator \hat{A}_{aA} in Eq. (48) is
 403 replaced by $\left(\begin{matrix} A \\ a \end{matrix}\right)^{1/2}$, one gets the equation for the radial overlap
 404 function with the source term $Q_{l_B j_B J_a J_A J_B}(r_{aA})$ [22]:

$$\begin{aligned} (E_{aA(0)} - \hat{T}_{r_{aA}} - V_{l_B}^{\text{centr}} - U_{aA}^C) I_{aA l_B j_B J_B}^B(r_{aA}) \\ = Q_{l_B j_B J_a J_A J_B}(r_{aA}). \end{aligned} \quad (49)$$

405 Here $\hat{T}_{r_{aA}}$ is the radial relative kinetic energy operator of the
 406 particles a and A , and $V_{l_B}^{\text{centr}}$ is the centrifugal barrier for the
 407 relative motion of a and A with the orbital momentum l_B . For
 408 charged particles it is convenient to single out the channel
 409 Coulomb interaction $U_{aA}^C(r_{aA})$ between the centers of mass of
 410 nuclei a and A .

The source term is given by

$$\begin{aligned} Q_{l_B j_B J_a J_A J_B}(r_{aA}) = \sum_{m_j m_B M_A M_a} \langle J_A M_A j_B m_j | J_B M_B \rangle \langle J_a M_a l_B m_l | j_B m_j \rangle \\ \times \left(\begin{matrix} A \\ a \end{matrix}\right)^{1/2} \int d\Omega_{\mathbf{r}_{aA}} \langle \varphi_a(\xi_a) \varphi_A(\xi_A) | V_{aA} - U_{aA}^C | Y_{l_B m_l}^*(\hat{\mathbf{r}}_{aA}) \Psi(\xi_a, \xi_A; \mathbf{r}_{aA}) \rangle. \end{aligned} \quad (50)$$

411 The integration in the matrix element $\langle \varphi_a(\xi_a) \varphi_A(\xi_A) | V_{aA} - U_{aA}^C | Y_{l_B m_l}^*(\hat{\mathbf{r}}_{aA}) \Psi(\xi_a, \xi_A; \mathbf{r}_{aA}) \rangle$ in Eq. (50) is carried out over all the
 412 internal coordinates of nuclei a and A .

413 Owing to the presence of the short-range potential operator $V_{aA} - U_{aA}^C$ (potential V_{aA} is the sum of the nuclear V_{aA}^N and the
 414 Coulomb V_{aA}^C potentials and subtraction of U_{aA}^C removes the long-range Coulomb term from V_{aA}) the source term is also a
 415 short-range function. Then Eq. (49) for the radial overlap function can be rewritten as
 416

$$I_{aA l_B j_B J_B}(k_{aA(0)}, r_{aA}) = \frac{1}{R_{aA}} \int_0^{R_{aA}} dr'_{aA} r'_{aA} G_{l_B}^C(r_{aA}, r'_{aA}; E_{aA(0)}) Q_{l_B j_B J_a J_A J_B}(r'_{aA}), \quad (51)$$

417 where R_{aA} is the $a - A$ nuclear interaction radius. In the R -matrix approach R_{aA} can be replaced by the channel radius R_{ch} , which
 418 can be varied.

419 Equation (51) is of fundamental importance because it allows one to express the radial overlap function in terms of the internal
 420 wave function of the nucleus B .

421 The partial Coulomb two-body Green function is given by [23]

$$G_{l_B}^C(r_{aA}, r'_{aA}; E_{aA}) = -2 \mu_{aA} \frac{\varphi_{l_B}^C(k_{aA}, r_{aA <}) f_{l_B}^{C(+)}(k_{aA}, r_{aA >})}{L_{l_B}^{C(+)}}, \quad (52)$$

422 where $r_{aA <} = \min\{r_{aA}, r'_{aA}\}$ and $r_{aA >} = \max\{r_{aA}, r'_{aA}\}$. The Coulomb regular solution $\varphi_{l_B}^C(k_{aA}, r_{aA})$ of the partial Schrödinger
 423 equation at real momentum k_{aA} is

$$\begin{aligned} \varphi_{l_B}^C(k_{aA}, r_{aA}) &= \frac{1}{2 i k_{aA}} [L_{l_B}^{C(-)}(k_{aA}) f_{l_B}^{C(+)}(k_{aA}, r_{aA}) - L_{l_B}^{C(+)}(k_{aA}) f_{l_B}^{C(-)}(k_{aA}, r_{aA})] \\ &= r_{aA}^{l_B+1} e^{i k_{aA} r_{aA}} {}_1F_1(l_B + 1 + i \eta_{aA}, 2 l_B + 2; -2 i k_{aA} r_{aA}) \\ &= e^{-i \pi l_B/2} L_{l_B}^{C(+)}(k_{aA}) \frac{e^{i \sigma_{l_B}^C} F_{l_B}(k_{aA}, r_{aA})}{k_{aA}}, \end{aligned} \quad (53)$$

424 where

$$e^{i \sigma_{l_B}^C} F_{l_B}(k_{aA}, r_{aA}) = e^{-\pi \eta_{aA}/2} \frac{\Gamma(l_B + 1 + i \eta_{aA})}{2 \Gamma(2 l_B + 2)} (2 k_{aA} r_{aA})^{l_B+1} e^{i k_{aA} r_{aA}} {}_1F_1(l_B + 1 + i \eta_{aA}, 2 l_B + 2; -i 2 k_{aA} r_{aA}), \quad (54)$$

425 $\sigma_{l_B}^C$ is the Coulomb scattering phase shift. Also

$$f_{l_B}^{C(\pm)}(k_{aA}, r_{aA}) = e^{\pi \eta_{aA}/2} W_{\mp i \eta_{aA}, l_B+1/2}(\mp 2 i k_{aA} r_{aA}) \quad (55)$$

426 are the Jost solutions (singular at the origin $r_{aA} = 0$),

$$L_{l_B}^{C(\pm)}(k_{aA}) = \frac{1}{(2 k_{aA})^{l_B}} e^{\pi \eta_{aA}/2} e^{\pm i \pi l_B/2} \frac{\Gamma(2 l_B + 2)}{\Gamma(l_B + 1 \pm i \eta_{aA})} \quad (56)$$

427 are the Jost functions.

428 It is convenient to introduce the modified Coulomb wave function

$$\tilde{\varphi}_{l_B}^C(k_{aA}, r_{aA}) = \frac{\varphi_{l_B}^C(k_{aA}, r_{aA})}{L_{l_B}^{C(+)}(k_{aA})}, \quad (57)$$

429 which will be used from now on instead of $\varphi_{l_B}^C(k_{aA}, r_{aA})$.

430 Let me use now the R -matrix method in which I replace R_{aA} by R_{ch} . Then assuming in Eq. (51) $r_{aA} = R_{\text{ch}} + i0$ and taking
 431 into account Eqs. (46) and (55) one gets

$$\tilde{C}_{l_B} = i^{-l_B} e^{-i[\delta_{l_B}^{\text{hs}} - \sigma_{l_B}^C]} \sqrt{\frac{\mu_{aA}}{k_{aA(0)}} \Gamma_{aA l_B j_B J_B}} = 2 \mu_{aA} \int_0^{R_{\text{ch}}} dr'_{aA} r'_{aA} \tilde{\varphi}_{l_B}^C(k_{aA(0)}, r'_{aA}) Q_{l_B j_B J_a J_A J_B}(r'_{aA}). \quad (58)$$

432 Using Eqs. (53) and (57) one gets

$$e^{-i \delta_{l_B}^{\text{hs}}} \sqrt{\frac{\mu_{aA}}{k_{aA(0)}} \Gamma_{aA l_B j_B J_B}} = 2 \frac{\mu_{aA}}{k_{aA(0)}} \int_0^{R_{\text{ch}}} dr'_{aA} r'_{aA} F_{l_B}(k_{aA(0)}, r'_{aA}) Q_{l_B j_B J_a J_A J_B}(r'_{aA}). \quad (59)$$

433 This equation provides the ANC or resonance width of the narrow resonance, which may depend on the channel radius R_{ch} .
 434 Here I am interested in the ratio of the resonance width and the square of the ANC of the mirror resonant and bound state. The
 435 sensitivity of this ratio to the variation of the channel radius is checked below.

436 B. ANC in terms of Wronskian

437 The advantage of Eq. (59) is that to calculate the ANC one needs to know the microscopic resonant wave functions only
 438 in the nuclear interior where the *ab initio* methods like the no-core shell model [24–26] and the coupled-cluster method [27]
 439 are more accurate than in the external region. That is why Eq. (59) is so important if microscopic resonant wave functions are
 440 available. Now I show that the radial integral in Eq. (59) can be transformed into the Wronskian at $r_{aA} = R_{aA}$. The philosophy
 441 of this transformation is the same as in the surface integral formalism [5, 11].

442 First, let us rewrite

$$V_{aA} - U_{aA}^C = V + V_{l_B}^{\text{centr}} - V_a - V_A - V_{l_B}^{\text{centr}} - U_{aA}^C \quad (60)$$

443 and take into account the equations

$$(E_{aA(0)} - \hat{T}_a - \hat{T}_A - \hat{T}_{r_{aA}}) \tilde{\varphi}_{l_B}^C(k_{aA(0)}, r_{aA}) \varphi_a(\xi_a) \varphi_A(\xi_A) = (U_{aA}^C + V_{l_B}^{\text{centr}} + V_a + V_A) \tilde{\varphi}_{l_B}^C(k_{aA(0)}, r_{aA}) \tilde{\varphi}_a(\xi_a) \varphi_A(\xi_A) \quad (61)$$

444 and

$$(E_{aA(0)} - \hat{T}_a - \hat{T}_A - \hat{T}_{r_{aA}}) \langle Y_{l_B m_{l_B}}(\hat{\mathbf{r}}_{aA}) | \Psi(\xi_a, \xi_A; \mathbf{r}_{aA}) \rangle = (V_{aA} + V_a + V_A + V_{l_B}^{\text{centr}}) \langle Y_{l_B m_{l_B}}(\hat{\mathbf{r}}_{aA}) | \Psi(\xi_a, \xi_A; \mathbf{r}_{aA}) \rangle, \quad (62)$$

445 where $\hat{T}_{r_{aA}}$ is the radial kinetic energy operator.

446 Then we get

$$\begin{aligned} \tilde{C}_{aA l_B j_B J_B}^B &\approx -2 \mu_{aA} \int_0^{R_{aA}} dr_{aA} r_{aA} \tilde{\varphi}_{l_B}^C(k_{aA(0)}, r_{aA}) Q_{l_B j_B J_a J_A J_B}(r_{aA}) \\ &= -2 \mu_{aA} \sum_{m_{j_B} m_{l_B} M_A M_a} \langle J_A M_A j_B m_{j_B} | J_B M_B \rangle \langle J_a M_a l_B m_{l_B} | j_B m_{j_B} \rangle \binom{A}{a}^{1/2} \int_0^{R_{aA}} dr_{aA} r_{aA} \tilde{\varphi}_{l_B}^C(k_{aA(0)}, r_{aA}) \\ &\quad \times \int d\Omega_{\mathbf{r}_{aA}} \langle \varphi_a(\xi_a) \varphi_A(\xi_A) | \overleftarrow{\hat{T}}_{r_{aA}} + \overleftarrow{\hat{T}}_a + \overleftarrow{\hat{T}}_A - \overrightarrow{\hat{T}}_a - \overrightarrow{\hat{T}}_A - \overrightarrow{\hat{T}}_{r_{aA}} | Y_{l_B m_{l_B}}^*(\hat{\mathbf{r}}_{aA}) \Psi(\xi_a, \xi_A; \mathbf{r}_{aA}) \rangle \\ &= -2 \mu_{aA} \sum_{m_{j_B} m_{l_B} M_A M_a} \langle J_A M_A j_B m_{j_B} | J_B M_B \rangle \langle J_a M_a l_B m_{l_B} | j_B m_{j_B} \rangle \\ &\quad \times \binom{A}{a}^{1/2} \int_0^{R_{aA}} dr_{aA} r_{aA} \tilde{\varphi}_{l_B}^C(k_{aA(0)}, r_{aA}) \int d\Omega_{\mathbf{r}_{aA}} \langle \varphi_a(\xi_a) \varphi_A(\xi_A) | \overleftarrow{\hat{T}}_{r_{aA}} - \overrightarrow{\hat{T}}_{r_{aA}} | Y_{l_B m_{l_B}}^*(\hat{\mathbf{r}}_{aA}) \Psi(\xi_a, \xi_A; \mathbf{r}_{aA}) \rangle \\ &= -2 \mu_{aA} \int_0^{R_{aA}} dr_{aA} r_{aA} \tilde{\varphi}_{l_B}^C(k_{aA(0)}, r_{aA}) (\overleftarrow{\hat{T}}_{r_{aA}} - \overrightarrow{\hat{T}}_{r_{aA}}) I_{aA l_B j_B J_B}(k_{aA(0)}, r_{aA}). \end{aligned} \quad (63)$$

447 Here R_{aA} is the $a - A$ nuclear interaction radius. In the R -matrix approach R_{aA} can be replaced by the channel radius R_{ch} which
448 can be varied.

449 Taking into account that

$$f(x) \left(\frac{\overleftarrow{d}^2}{dx^2} - \frac{\overrightarrow{d}^2}{dx^2} \right) g(x) = \frac{d}{dx} \left(g(x) \frac{df(x)}{dx} - f(x) \frac{dg(x)}{dx} \right) \quad (64)$$

450 we arrive at the final expression for the ANC of the resonance state in terms of the Wronskian:

$$\tilde{C}_{aA l_B j_B J_B}^B = \mathcal{W}[I_{aA l_B j_B J_B}(k_{aA(0)}, r_{aA}), \tilde{\varphi}_{l_B}^C(k_{aA(0)}, r_{aA})] \Big|_{r_{aA}=R_{\text{ch}}}, \quad (65)$$

451 where the Wronskian

$$\begin{aligned} &\mathcal{W}[I_{aA l_B j_B J_B}(r_{aA}), \tilde{\varphi}_{l_B}^C(k_{aA(0)}, r_{aA})] \\ &= I_{aA l_B j_B J_B}(k_{aA(0)}, r_{aA}) \frac{d\tilde{\varphi}_{l_B}^C(k_{aA(0)}, r_{aA})}{dr_{aA}} - \tilde{\varphi}_{l_B}^C(k_{aA(0)}, r_{aA}) \frac{dI_{aA l_B j_B J_B}(k_{aA(0)}, r_{aA})}{dr_{aA}}. \end{aligned} \quad (66)$$

452 I would like to underscore that Eq. (65) was derived by transforming the internal integral into the Wronskian at the channel radius
453 R_{ch} . Note that at too small radii R_{ch} the Wronskian $\mathcal{W}[I_{aA l_B j_B J_B}(r_{aA}), \tilde{\varphi}_{l_B}^C(k_{aA(0)}, r_{aA})]$ depends on the radius but the sensitivity
454 to the radius decreases as R_{ch} increases.

455 There is another more direct derivation of Eq. (65). We know that the Wronskian calculated for two independent solutions of
456 the Schrödinger equation is a constant [23]. In the R -matrix approach the internal radial overlap function $I_{aA l_B j_B J_B}(k_{aA(0)}, r_{aA})$ at
457 $r_{aA} \rightarrow R_{\text{ch}}$ behaves like the Whittaker function [see Eq. (46)] and is given by

$$I_{aA l_B j_B J_B}(k_{aA(0)}, r_{aA}) = \tilde{C}_{aA l_B j_B J_B}^B \frac{f_{l_B}^{C(+)}(k_{aA(0)}, r_{aA})}{R_{\text{ch}}}. \quad (67)$$

This Whittaker function is a singular solution of the radial Schrödinger equation. $\tilde{\varphi}_{l_B}^C(k_{aA(0)}, r_{aA})$ is an independent regular solution of the same equation. Taking into account that $\mathcal{W}[f_{l_B}^{C(+)}(k_{aA(0)}, r_{aA}), f_{l_B}^{C(-)}(k_{aA(0)}, r_{aA})] = -2i k_{aA(0)}$ and Eq. (53) one gets at $r_{aA} = R_{ch}$

$$\mathcal{W}[I_{aA l_B j_B J_B}(k_{aA(0)}, r_{aA}), \tilde{\varphi}_{l_B}^C(k_{aA(0)}, r_{aA})] \Big|_{r_{aA}=R_{ch}} = \tilde{C}_{aA l_B j_B J_B}^B. \quad (68)$$

Note that the constancy of the Wronskian only applies to local potentials. But here one needs this only at large distances, where zero potentials are local anyway.

I demonstrate that the Wronskian $\mathcal{W}[I_{aA l_B j_B J_B}(k_{aA(0)}, r_{aA}), \tilde{\varphi}_{l_B}^C(k_{aA(0)}, r_{aA})] \Big|_{r_{aA}=R_{ch}}$ depends on R_{ch} and reaches a constant value, which is equal to the ANC of the resonance state, when R_{ch} increases.

My idea is to use Eq. (65) to calculate the Wronskian $\mathcal{W}[I_{aA l_B j_B J_B}(k_{aA(0)}, r_{aA}), \tilde{\varphi}_{l_B}^C(k_{aA(0)}, r_{aA})] \Big|_{r_{aA}=R_{ch}}$ at the channel radii which are smaller than the radius of nucleus $B = (aA)$, and gradually increase R_{ch} until the Wronskian reaches its constant value. In the nuclear interior the contemporary

microscopic models can provide quite accurate overlap functions. The sensitivity to the variation of the channel radius of the ratio of the ANCs of the resonance and mirror bound state is significantly weaker than that of the individual ANCs (or, equivalently, of the resonance width and the bound-state ANC) of the mirror states.

VI. RATIO OF RESONANCE WIDTH AND ANC OF MIRROR BOUND STATE

A. Three different equations

In this part three different equations for the ratio of the resonance width and the ANC of the mirror bound state are presented. Let $B_1 = (a_1 A_1)$ and $B_2 = (a_2 A_2)$ be mirror nuclei. Then the quantum numbers in both nuclei are the same. We also assume that the channel radius R_{ch} is the same for both mirror nuclei. The ratio of the ANCs of the mirror resonance and bound states is given by the ratio of the corresponding Wronskians. Taking into account Eq. (65) one gets for the ratio of the resonance width and the bound state ANC for mirror states

$$\frac{\Gamma_{a_1 A_1 l_B j_B J_B}}{(C_{a_2 A_2 l_B j_B J_B}^{B_2})^2} = \sqrt{\frac{2 E_{a_1 A_1(0)}}{\mu_{a_1 A_1}}} \frac{|\mathcal{W}[I_{a_1 A_1 l_B j_B J_B}(k_{a_1 A_1(0)}, r_{a_1 A_1}), \tilde{\varphi}_{l_B}^C(k_{a_1 A_1(0)}, r_{a_1 A_1})] \Big|_{r_{a_1 A_1}=R_{ch}}}{(\mathcal{W}[I_{a_2 A_2 l_B j_B J_B}(\kappa_{a_2 A_2}, r_{a_2 A_2}), \tilde{\varphi}_{l_B}^C(i\kappa_{a_2 A_2}, r_{a_2 A_2})] \Big|_{r_{a_2 A_2}=R_{ch}})^2}, \quad (69)$$

where $E_{a_1 A_1(0)}$ and μ_{aA} are expressed in MeV. Equation (69) allows one to determine the resonance width if the ANC of the mirror bound state is known and vice versa.

To calculate the ratio $\frac{\Gamma_{a_1 A_1 l_B j_B J_B}}{(C_{a_2 A_2 l_B j_B J_B}^{B_1})^2}$ one needs the microscopic radial overlap functions. If these radial overlap functions are not available then one can use a standard approximation for the overlap functions:

$$I_{a_1 A_1 l_B j_B J_B}(k_{a_1 A_1(0)}, r_{aA}) \approx S_{a_1 A_1}^{1/2} \varphi_{a_1 A_1 l_B j_B J_B}(k_{a_1 A_1(0)}, r_{a_1 A_1}), \quad (70)$$

$$I_{a_2 A_2 l_B j_B J_B}(\kappa_{a_2 A_2}, r_{aA}) \approx S_{a_2 A_2}^{1/2} \varphi_{a_2 A_2 l_B j_B J_B}(\kappa_{a_2 A_2}, r_{a_2 A_2}), \quad (71)$$

where $S_{a_1 A_1}$ and $S_{a_2 A_2}$ are the spectroscopic factors of the mirror resonance and bound states $(a_1 A_1)$ and $(a_2 A_2)$, respectively. $\varphi_{a_1 A_1 l_B j_B J_B}(k_{a_1 A_1(0)}, r_{a_1 A_1})$ is a real internal resonant wave function calculated in the two-body model $(a_1 A_1)$ using some phenomenological potential, for example, a Woods-Saxon one, which supports the resonance state under consideration. $\varphi_{a_2 A_2 l_B j_B J_B}(\kappa_{a_2 A_2}, r_{a_2 A_2})$ is the two-body bound-state wave function of the bound state $(a_2 A_2)$, which is also calculated using the same nuclear potential as the mirror resonance state. If the mirror symmetry holds then $S_{a_1 A_1} \approx S_{a_2 A_2}$ and one gets an approximated $\frac{\Gamma_{a_1 A_1 l_B j_B J_B}}{(C_{a_2 A_2 l_B j_B J_B}^{B_2})^2}$ ratio in terms of the Wronskians, which does not contain the overlap functions:

$$\frac{\Gamma_{a_1 A_1 l_B j_B J_B}}{(C_{a_2 A_2 l_B j_B J_B}^{B_2})^2} \approx \sqrt{\frac{2 E_{a_1 A_1(0)}}{\mu_{a_1 A_1}}} \frac{|\mathcal{W}[\varphi_{a_1 A_1 l_B j_B J_B}(k_{a_1 A_1(0)}, r_{a_1 A_1}), \tilde{\varphi}_{l_B}^C(k_{a_1 A_1(0)}, r_{a_1 A_1})] \Big|_{r_{a_1 A_1}=R_{ch}}}{(\mathcal{W}[\varphi_{a_2 A_2 l_B j_B J_B}(\kappa_{a_2 A_2}, r_{a_2 A_2}), \tilde{\varphi}_{l_B}^C(i\kappa_{a_2 A_2}, r_{a_2 A_2})] \Big|_{r_{a_2 A_2}=R_{ch}})^2}. \quad (72)$$

Meanwhile in Ref. [10] another expression for the mirror nucleon ANCs ratio was obtained which provides the easiest way to determine $\frac{\Gamma_{a_1 A_1 l_B j_B J_B}}{(C_{a_2 A_2 l_B j_B J_B}^{B_2})^2}$. I show here a simple way of the derivation of the ratio $\frac{\Gamma_{a_1 A_1 l_B j_B J_B}}{(C_{a_2 A_2 l_B j_B J_B}^{B_2})^2}$ from Ref. [10]. First, as it was pointed out in Ref. [10], in the nuclear interior the Coulomb interaction varies very little in the nuclear interior and its effect leads only to shifting of the energy of the bound state to the continuum. Hence, it can be assumed that $\tilde{\varphi}_{l_B}^C(k_{a_1 A_1(0)}, r_{a_1 A_1})$ and $\tilde{\varphi}_{l_B}^C(i\kappa_{a_2 A_2}, r_{a_2 A_2})$ behave similarly in the nuclear interior except for the overall normalization; that is,

$$\tilde{\varphi}_{l_B}^C(k_{a_1 A_1(0)}, r_{aA}) = \frac{\tilde{\varphi}_{l_B}^C(k_{a_1 A_1(0)}, R_{ch})}{\tilde{\varphi}_{l_B}^C(i\kappa_{a_2 A_2}, R_{ch})} \tilde{\varphi}_{l_B}^C(i\kappa_{a_2 A_2}, r_{a_2 A_2}). \quad (73)$$

Then

$$\frac{\Gamma_{a_1 A_1 l_B j_B J_B}}{(C_{a_2 A_2 l_B j_B J_B}^{B_2})^2} \approx \sqrt{\frac{2 E_{a_1 A_1(0)}}{\mu_{a_1 A_1}}} \left(\frac{\tilde{\varphi}_{l_B}^C(k_{a_1 A_1(0)}, R_{\text{ch}})}{\tilde{\varphi}_{l_B}^C(i \kappa_{a_2 A_2}, R_{\text{ch}})} \right)^2 \frac{|\mathcal{W}[\varphi_{a_1 A_1 l_B j_B J_B}(k_{a_1 A_1(0)}, r_{a_1 A_1}), \tilde{\varphi}_{l_B}^C(i \kappa_{a_2 A_2}, r_{a_2 A_2})]|^2 \Big|_{r_{a_1 A_1}, r_{a_2 A_2} = R_{\text{ch}}}}{(\mathcal{W}[\varphi_{a_2 A_2 l_B j_B J_B}(\kappa_{a_2 A_2}, r_{a_2 A_2}), \tilde{\varphi}_{l_B}^C(i \kappa_{a_2 A_2}, r_{a_2 A_2})])^2 \Big|_{r_{a_2 A_2} = R_{\text{ch}}}}. \quad (74)$$

Neglecting further the difference between the mirror wave functions $\varphi_{a_1 A_1 l_B j_B J_B}(k_{a_1 A_1(0)}, r_{a_1 A_1})$ and $\varphi_{a_2 A_2 l_B j_B J_B}(\kappa_{a_2 A_2}, r_{a_2 A_2})$ in the nuclear interior we obtain the approximate expression for $\frac{\Gamma_{a_1 A_1 l_B j_B J_B}}{(C_{a_2 A_2 l_B j_B J_B}^{B_2})^2}$ from Ref. [10] (in the notations of the current paper):

$$\frac{\Gamma_{a_1 A_1 l_B j_B J_B}}{(C_{a_2 A_2 l_B j_B J_B}^{B_2})^2} \approx \sqrt{\frac{2 E_{a_1 A_1(0)}}{\mu_{a_1 A_1}}} \left(\frac{\tilde{\varphi}_{l_B}^C(k_{a_1 A_1(0)}, R_{\text{ch}})}{\tilde{\varphi}_{l_B}^C(i \kappa_{a_2 A_2}, R_{\text{ch}})} \right)^2. \quad (75)$$

In descending accuracy, Eq. (69) is ranked as the most accurate. Taking into account that the microscopic overlap functions (calculated in the no-core shell model [24–26] or oscillator shell model [28]) are accurate in the nuclear interior, using Eq. (69) one can determine the ratio $\frac{\Gamma_{a_1 A_1 l_B j_B J_B}}{(C_{a_2 A_2 l_B j_B J_B}^{B_2})^2}$ quite accurately. Then follows Eq. (72) and finally Eq. (75). Note that Eq. (75) is valid only in the region where the mirror resonant and bound-state wave functions do coincide or are very close. The advantage of this equation is that it allows one to calculate the ratio without using the mirror wave functions and it is extremely simple to use.

Because for the cases under consideration the internal microscopic resonance wave functions are not available, in this paper the $\frac{\Gamma_{a_1 A_1 l_B j_B J_B}}{(C_{a_2 A_2 l_B j_B J_B}^{B_2})^2}$ ratio is calculated using Eqs. (72) and (75). It allows one to determine the accuracy of both equations.

Note that the dimension of the ratio $\frac{\Gamma_{a_1 A_1 l_B j_B J_B}}{(C_{a_2 A_2 l_B j_B J_B}^{B_2})^2}$ is determined by the ratio $\frac{2 E_{a_1 A_1(0)}}{\mu_{a_1 A_1}}$. To make it dimensionless I assume that the reduced mass $\mu_{a_1 A_1}$ and the real part of the resonance energy $E_{a_1 A_1(0)}$ are expressed in MeV.

B. *R*-matrix wave function

Because the microscopic overlap functions for mirror resonances are not available, in this paper I use internal resonance and bound-state wave functions calculated in the potential model at real energies. In the developed Wronskian method one needs the wave functions in the internal region in which it is very convenient to use the *R*-matrix method. In the *R*-matrix approach the resonant wave function is considered at the real part of the resonance energy $E_{aA(0)}$ and is real in the internal region. If the mirror symmetry holds, the bound-state and resonance wave functions of the mirror states should be very similar in the internal region. The *R*-matrix resonant wave function is normalized to unity in the internal region. The border of this region is determined by the point at which the radial derivative of the internal resonant wave function is equal to zero. If the resonant wave function has a few nodes, the border of the internal region is determined by the last point at which the radial derivative of the resonant wave function vanishes. The bound-state wave function is normalized to

unity in the whole coordinate space. To make the bound-state wave function close to the resonant wave function the former is also renormalized to unity in the internal region. The advantage of the Wronskian method is that to calculate the ratio of the resonance width and the ANC of the mirror states one can use the internal real resonant and bound-state wave functions.

VII. COMPARISON OF RESONANCE WIDTHS AND ANCS OF MIRROR STATES

In this section a few examples of the application of Eqs. (72) and (75) are presented. To simplify the notations from now on the quantum numbers in the notations for the resonance width and the ANC are dropped and just use simplified notations, $\Gamma_{a_1 A_1}$ and $C_{a_2 A_2}$. Equation (72) gives $\Gamma_{a_1 A_1}/(C_{a_2 A_2})^2$ in terms of the ratio of the Wronskians and provides an exact value for given two-body mirror resonant and bound-state wave functions. Equation (75) gives the $\Gamma_{a_1 A_1}/(C_{a_2 A_2})^2$ ratio in terms of the Coulomb scattering wave functions at the real resonance momentum $k_{a_1 A_1(0)}$ and the imaginary momentum of the bound state $i \kappa_{a_2 A_2}$ at the channel radius R_{ch} . Hence, to determine the ratio $\Gamma_{a_1 A_1}/(C_{a_2 A_2})^2$ using Eq. (75) one does not need to know the mirror resonant and bound-state wave functions. However, to use this equation one should check whether the mirror wave functions are close. In calculations I deliberately increase the channel radius R_{ch} to demonstrate the convergence of the calculated ratio $\Gamma_{a_1 A_1}/(C_{a_2 A_2})^2$ as R_{ch} increases.

A. Comparison of resonance width for

$^{13}\text{N}(2s_{1/2}) \rightarrow ^{12}\text{C}(0.0 \text{ MeV}) + p$ and mirror ANC for virtual decay $^{13}\text{C}(2s_{1/2}) \rightarrow ^{12}\text{C}(0.0 \text{ MeV}) + n$

I begin from the analysis of the isobaric analog states $2s_{1/2}$ in the mirror nuclei ^{13}N and ^{13}C . The resonance energy of $^{13}\text{N}(2s_{1/2})$ is $E_{p^{12}\text{C}(0)} = 0.421 \text{ MeV}$ with the resonance width of $\Gamma_{p^{12}\text{C}} = 0.0317 \pm 0.0008 \text{ MeV}$ [29]. The neutron binding energy of the mirror state $^{13}\text{C}(2s_{1/2})$ is $E_{n^{12}\text{C}} = 1.8574 \text{ MeV}$ with the experimental ANC $C_{n^{12}\text{C}} = 3.65 \text{ fm}^{-1}$ [30,31]. The experimental ratio $\Gamma_{p^{12}\text{C}}/(C_{n^{12}\text{C}})^2 = (4.40 \pm 0.57) \times 10^{-5}$ allows us to check the accuracy of both used equations. Because the dimension of the bound-state ANC is $\text{fm}^{-1/2}$ to get the dimensionless ratio I calculated $\Gamma_{p^{12}\text{C}}/[\hbar c(C_{n^{12}\text{C}})^2]$.

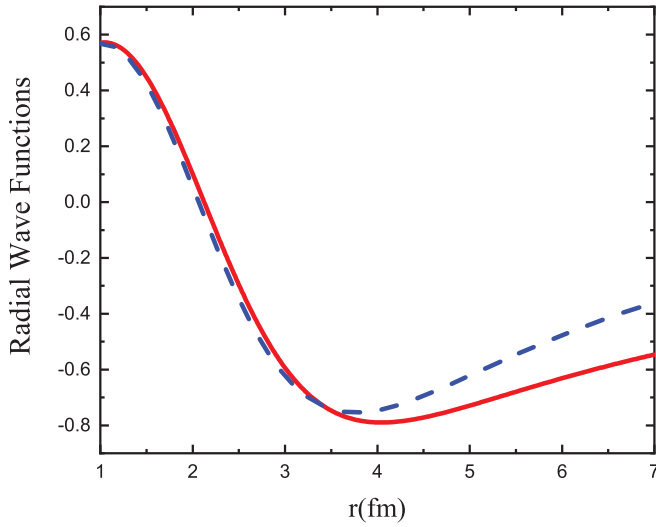


FIG. 1. Solid red line, the radial wave function of the $(p^{12}\text{C})_{2s^1/2}$ resonance state; dashed blue line, the radial wave function of the mirror $(n^{12}\text{C})_{2s^1/2}$ bound state. r is the distance between N , where $N = p, n$, and the c.m. of ^{12}C .

In Fig. 1 are shown the radial wave functions of the mirror states. Following the R -matrix procedure, both wave functions are normalized to unity over the internal volume with the radius $R_{\text{ch}} = 4.0$ fm. We see that the mirror wave functions are very close at distances ≤ 4.0 fm, which confirms the mirror symmetry of $(p^{12}\text{C})_{2s^1/2}$ and $(n^{12}\text{C})_{2s^1/2}$ systems.

In Fig. 2 are shown the $\frac{\Gamma_{p^{12}\text{C}}}{(C_{n^{12}\text{C}})^2}$ ratios, which are calculated using Eqs. (72) and (75). These calculated ratios are compared with the experimental one. We see that the calculations exceed the experimental value. The $\frac{\Gamma_{p^{12}\text{C}}}{(C_{n^{12}\text{C}})^2}$ ratio calculated using the simplified Eq. (75) shows the R_{ch} dependence and is equal to 10.13×10^{-5} at the peak at $R_{\text{ch}} = 5.22$ fm.

Equation (72) provides the $\frac{\Gamma_{p^{12}\text{C}}}{(C_{n^{12}\text{C}})^2}$ ratio in terms of the ratio of the Wronskians. Each Wronskian contains the two-body wave function and its radial derivative of the system $(N^{12}\text{C})_{2s^1/2}$, $N = p, n$. Each two-body wave function has one node at $r \approx 2.13$ fm and a minimum at $r \approx 4.0$ fm. Hence, at some point r the Wronskian in the denominator of Eq. (72) vanishes causing a discontinuity in the ratio $\frac{\Gamma_{p^{12}\text{C}}}{(C_{n^{12}\text{C}})^2}$. I assume that in the nuclear interior the mirror two-body wave functions are correct (as it should be for the mirror microscopic overlap functions) and calculate the ratio at $E_{\text{ch}} \geq 4$ fm. At $r = 4$ fm $\frac{\Gamma_{p^{12}\text{C}}}{(C_{n^{12}\text{C}})^2} = 8.1 \times 10^{-5}$ while the correct value of this ratio obtained at large R_{ch} is 9.8×10^{-5} , which is close to the peak value of the ratio obtained using Eq. (75).

Both used equations provide the values of the $\frac{\Gamma_{p^{12}\text{C}}}{(C_{n^{12}\text{C}})^2}$ ratio, which exceed the experimental one. It means that more accurate internal overlap functions are required and the two-body wave functions used here demonstrate the accuracy of the Wronskian method. However, there is another important

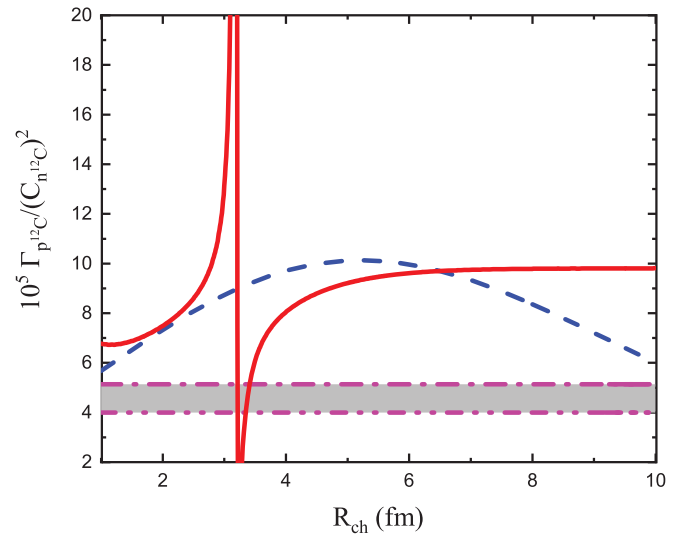


FIG. 2. The grey band is the experimental $\frac{\Gamma_{p^{12}\text{C}}}{(C_{n^{12}\text{C}})^2}$ ratio of the resonance width of the resonance state $^{13}\text{N}(2s^1/2)$ and the ANC of the mirror bound state $^{13}\text{C}(2s^1/2)$; the red dash-dot-dotted line and the red dash-dotted lines are the low and upper limits of this experimental ratio; the solid red line is the $\frac{\Gamma_{p^{12}\text{C}}}{(C_{n^{12}\text{C}})^2}$ ratio as a function of R_{ch} calculated using Eq. (72); the blue dotted line is the $\frac{\Gamma_{p^{12}\text{C}}}{(C_{n^{12}\text{C}})^2}$ ratio calculated as a function of R_{ch} using Eq. (75).

conclusion: the simple Eq. (75) in the peak gives the same result as the asymptotic ratio given by Eq. (72).

B. Comparison of resonance width for $^{13}\text{N}(1d_{5/2}) \rightarrow ^{12}\text{C}(0.0 \text{ MeV}) + p$ and mirror ANC for virtual decay $^{13}\text{C}(1d_{5/2}) \rightarrow ^{12}\text{C}(0.0 \text{ MeV}) + n$

As the second example I consider the isobaric analog states $1d_{5/2}$ in the mirror nuclei ^{13}N and ^{13}C . The resonance energy of $^{13}\text{N}(1d_{5/2})$ is $E_{p^{12}\text{C}(0)} = 1.6065$ MeV with the resonance width of $\Gamma_{p^{12}\text{C}} = 0.047 \pm 0.0008$ MeV [29]. The neutron binding energy of the mirror state $^{13}\text{C}(1d_{5/2})$ is $\varepsilon_{n^{12}\text{C}} = 1.09635$ MeV with the experimental ANC $C_{n^{12}\text{C}}^2 = 0.0225 \text{ fm}^{-1}$ [30]. The experimental ratio is $\Gamma_{p^{12}\text{C}}/C_{n^{12}\text{C}}^2 = (1.1 \pm 0.2) \times 10^{-2}$.

In Fig. 3 are shown the radial wave functions of the mirror states. Following the R -matrix procedure, both wave functions are normalized to unity over the internal volume with the radius $R_{\text{ch}} = 3$ fm. We see that the mirror wave functions are very close at distances $r \leq 4$ fm, which confirms the mirror symmetry of $(p^{12}\text{C})_{1d^3/2}$ and $(n^{12}\text{C})_{1d^3/2}$ systems. In Fig. 4 are shown the $\frac{\Gamma_{p^{12}\text{C}}}{(C_{n^{12}\text{C}})^2}$ ratios calculated using Eqs. (72) and (75), which are compared with the experimental ratio. We see that the calculated ratios are closer to the experimental ratio than in the previous case and both equations give quite reasonable results. The $\frac{\Gamma_{p^{12}\text{C}}}{(C_{n^{12}\text{C}})^2}$ ratio calculated using the simplified Eq. (75) shows the R_{ch} dependence and is equal to 0.0141 at the peak at $R_{\text{ch}} = 3.95$ fm. In the case under consideration the bound-state wave function does not have nodes at $r > 0$. That

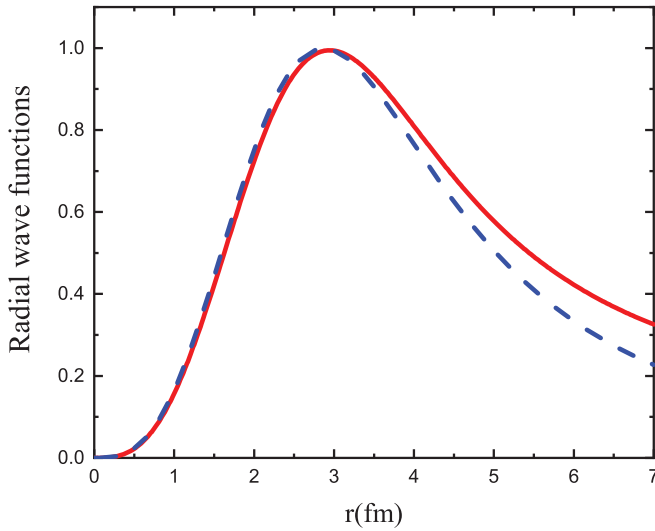


FIG. 3. Solid red line, the radial wave function of the $(p^{12}\text{C})_{1d_{5/2}^+}$ resonance state; dashed blue line, the radial wave function of the mirror $(n^{12}\text{C})_{1d_{5/2}^+}$ bound state. r is the distance between N , where $N = p, n$, and the c.m. of ^{12}C .

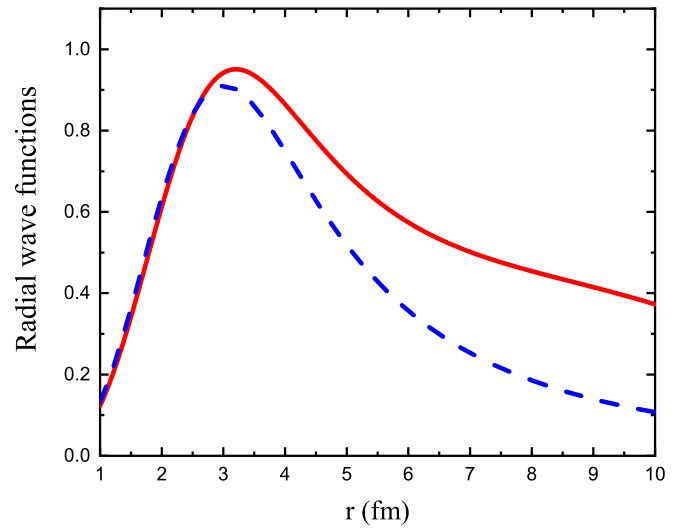


FIG. 5. Solid red line, the radial wave function of the $(p^{14}\text{O})_{1d_{5/2}}$ resonance state; dashed blue line, the radial wave function of the mirror $(n^{14}\text{C})_{1d_{5/2}}$ bound state. r is the distance between the nucleon and the c.m. of the nucleus.

650 is why the $\frac{\Gamma_{p^{12}\text{C}}}{(C_{n^{12}\text{C}})^2}$ ratio calculated using Eq. (72) is a smooth
 651 function of R_{ch} . This equation gives $\frac{\Gamma_{p^{12}\text{C}}}{(C_{n^{12}\text{C}})^2} = 0.0135$ at $R_{\text{ch}} =$
 652 4 fm, which differs very little from its correct asymptotic value
 653 of 0.0143. Again, as in the previous case, our calculations

show that the simple Eq. (75) can give the results close to the
 Wronskian method.

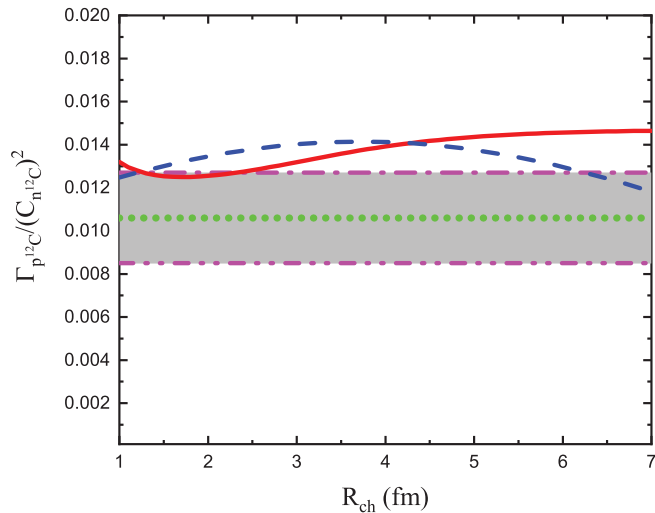


FIG. 4. The grey band is the experimental $\frac{\Gamma_{p^{12}\text{C}}}{(C_{n^{12}\text{C}})^2}$ ratio of the resonance width of the resonance state $^{13}\text{N}(1d_{5/2}^+)$ and the ANC of the mirror bound state $^{13}\text{C}(1d_{5/2}^+)$; the red dash-dot-dotted line and the red dash-dot lines are the low and upper limits of this experimental ratio; the green dotted line is the adopted experimental value of the ratio $\frac{\Gamma_{p^{12}\text{C}}}{(C_{n^{12}\text{C}})^2} = (1.1 \pm 0.2) \times 10^{-2}$; the solid red line is the $\frac{\Gamma_{p^{12}\text{C}}}{(C_{n^{12}\text{C}})^2}$ ratio as a function of R_{ch} calculated using Eq. (72); and the blue dotted line is the $\frac{\Gamma_{p^{12}\text{C}}}{(C_{n^{12}\text{C}})^2}$ ratio calculated as a function of R_{ch} using Eq. (75).

C. Comparison of resonance width for

$^{15}\text{F}(1d_{5/2}) \rightarrow ^{14}\text{O}(0.0 \text{ MeV}) + p$ and mirror ANC for virtual decay $^{15}\text{C}(1d_{5/2}) \rightarrow ^{14}\text{C}(0.0 \text{ MeV}) + n$

In this section I determine the ratio $\Gamma_{p^{14}\text{O}}/C_{n^{14}\text{C}}^2$ for the mirror states $^{15}\text{F}(1d_{5/2})$ and $^{15}\text{C}(1d_{5/2})$. The resonance energy and the resonance width of $^{15}\text{F}(1d_{5/2})$ are $E_{p^{14}\text{O}(0)} = 2.77 \text{ MeV}$ and $\Gamma_{p^{14}\text{O}} = 0.24 \pm 0.03 \text{ MeV}$ [32]. The binding energy and the ANC of the bound state $^{15}\text{C}(1d_{5/2})$ are $\varepsilon_{n^{14}\text{C}} = 0.478 \text{ MeV}$ and $C_{n^{14}\text{C}}^2 = (3.6 \pm 0.8) \times 10^{-3} \text{ fm}^{-1}$. The experimental ratio $\Gamma_{p^{14}\text{O}}/C_{n^{14}\text{C}}^2 = 0.338 \pm 0.001$.

This is the most difficult case because the resonance state is not potential. It is clear from Fig. 5.

The mirror wave functions are normalized in the internal region $r \leq 3.2 \text{ fm}$. They begin to deviate at $r > 3.0 \text{ fm}$. Because the resonance width in the case under consideration is much wider than in the previous cases, the resonant wave function calculated in the potential model in the external region differs significantly from the tail of the bound-state wave function. That is why the Wronskian ratio does not have an asymptote at large r . But the idea of the Wronskian method is to determine the $\Gamma_{p^{14}\text{O}}/C_{n^{14}\text{C}}^2$ ratio using the mirror wave functions in the internal region where they practically coincide.

In Fig. 6 is shown the $\Gamma_{p^{14}\text{O}}/C_{n^{14}\text{C}}^2$ ratio calculated using the Wronskian method and the simplified Eq. (75). The Wronskian ratio at 4.0 fm is 0.32 while Eq. (75) gives 0.31. Both values are very close to the experimental ratio.

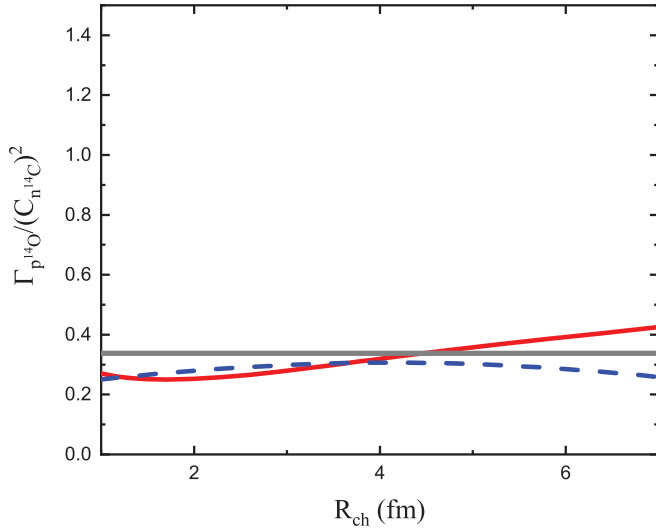


FIG. 6. The grey band is the experimental $\frac{\Gamma_{p^{14}O}}{(C_{n^{14}C})^2}$ ratio for the resonance state $^{15}\text{F}(1d_{5/2}^+)$ and the mirror bound state $^{15}\text{C}(1d_{5/2}^+)$; the solid red line is the $\frac{\Gamma_{p^{14}O}}{(C_{n^{14}C})^2}$ ratio as a function of R_{ch} calculated using Eq. (72); and the blue dashed line is the $\frac{\Gamma_{p^{14}O}}{(C_{n^{14}C})^2}$ ratio calculated as a function of R_{ch} using Eq. (75).

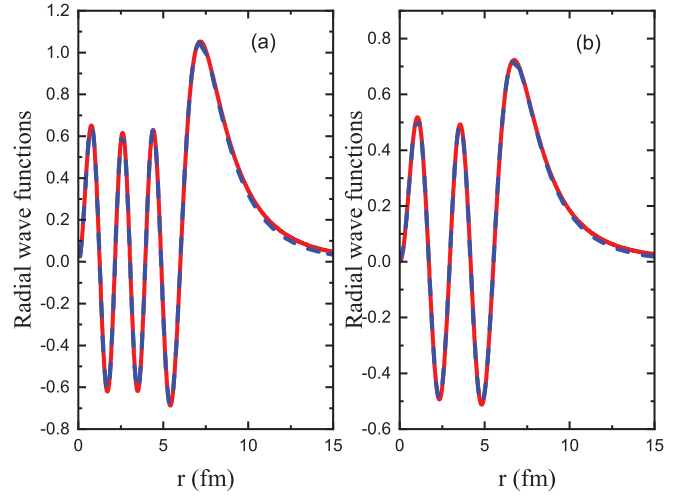


FIG. 7. (a) The mirror radial wave functions for $N = 6$: the solid red line is the $(\alpha^{14}\text{O})_1^-$ resonance wave function, and the dashed blue line is the radial wave function of the mirror $(\alpha^{14}\text{C})_1^-$ bound state. r is the distance between the α particle and the c.m. of the nucleus. (b) Notations are the same as in (a) but for $N = 4$.

D. Comparison of resonance width for $^{18}\text{Ne}(1^-) \rightarrow ^{14}\text{O}(0.0 \text{ MeV}) + \alpha$ and mirror ANC for virtual decay $^{18}\text{O}(1^-) \rightarrow ^{14}\text{C}(0.0 \text{ MeV}) + \alpha$

In this section I determine the ratio $\Gamma_{\alpha^{14}\text{O}}/C_{\alpha^{14}\text{C}}^2$ for the mirror states $^{18}\text{Ne}(1^-)$ and $^{18}\text{O}(1^-)$. The resonance energy is $E_{\alpha^{14}\text{O}(0)} = 1.038 \text{ MeV}$. The binding energy of the bound state $^{18}\text{O}(1^-)$ is $\varepsilon_{\alpha^{14}\text{C}} = 0.027 \text{ MeV}$. The resonance width and the ANC of the mirror states are unknown.

The purpose of this section is to show that the ratio $\Gamma_{\alpha^{14}\text{O}}/C_{\alpha^{14}\text{C}}^2$ does not depend on the number of the nodes of the mirror wave functions. The potential model search showed that for the given resonance energy and binding energy for $l = 1$ the mirror wave functions have at $r > 0$ the number of nodes $N = 4$ or 6 . The normalization region of the mirror wave functions is $r \leq 7.2 \text{ fm}$ for $N = 6$ and $r \leq 6.73 \text{ fm}$ for $N = 4$. In Figs. 7 and 8 are shown the radial wave functions and the ratio $\Gamma_{\alpha^{14}\text{O}}/C_{\alpha^{14}\text{C}}^2$ for the number of nodes $N = 4$ and 6 .

One can see that the mirror wave functions practically coincide up to $r = 15 \text{ fm}$. It means that the simplified Eq. (75) can be used up to 15 fm . The ratio $\Gamma_{\alpha^{14}\text{O}}/C_{\alpha^{14}\text{C}}^2$ calculated using Eq. (72) is the same for $N = 4$ and 6 . Because the mirror wave functions are practically identical in the external region the ratio $\Gamma_{\alpha^{14}\text{O}}/C_{\alpha^{14}\text{C}}^2$ calculated using the Wronskian method [Eq. (72)] has an asymptote. The calculated ratio for $N = 4, 6$ reaches its asymptotic value at $R_{\text{ch}} = 7.5 \text{ fm}$ which is $\Gamma_{\alpha^{14}\text{O}}/C_{\alpha^{14}\text{C}}^2 = 3.48 \times 10^{52}$. The maximum of $\Gamma_{\alpha^{14}\text{O}}/C_{\alpha^{14}\text{C}}^2$ calculated using Eq. (75) at $R_{\text{ch}} = 9 \text{ fm}$ is 3.42×10^{52} . This comparison demonstrates again that in the absence of the microscopic internal overlap functions both the Wronskian

and the simplified method given by Eq. (75) can be used and give very close results. 713 714

E. Comparison of resonance width for $^{17}\text{F}(s_{1/2}) \rightarrow ^{13}\text{N}(0.0 \text{ MeV}) + \alpha$ and mirror ANC for virtual decay $^{17}\text{O}(s_{1/2}) \rightarrow ^{13}\text{C}(0.0 \text{ MeV}) + \alpha$

The last case that I consider is the determination of the ratio $\frac{\Gamma_{\alpha^{13}\text{N}}}{(C_{\alpha^{13}\text{C}})^2}$ of the resonance state $^{17}\text{F}(1/2^+)$ and the mirror bound 718 719

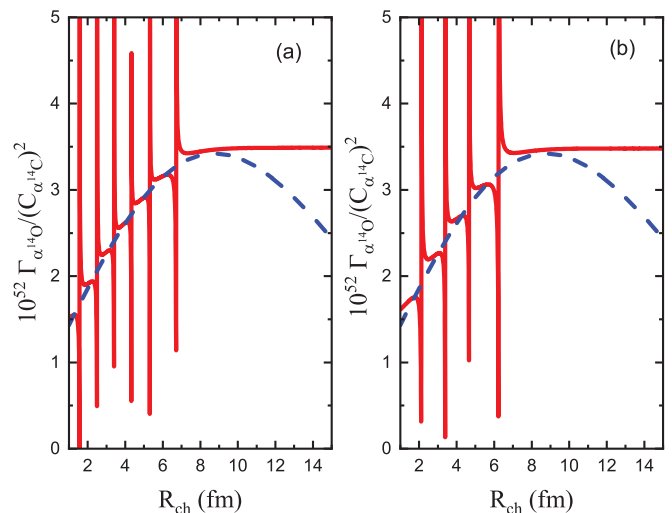


FIG. 8. (a) The $\frac{\Gamma_{\alpha^{14}\text{O}}}{(C_{\alpha^{14}\text{C}})^2}$ ratio for the resonance state $^{18}\text{Ne}(1^-)$ and the mirror bound state $^{18}\text{O}(1^-)$ for $N = 6$: the solid red line is the $\frac{\Gamma_{\alpha^{14}\text{O}}}{(C_{\alpha^{14}\text{C}})^2}$ ratio as a function of R_{ch} calculated using Eq. (72), and the blue dashed line is the $\frac{\Gamma_{\alpha^{14}\text{O}}}{(C_{\alpha^{14}\text{C}})^2}$ ratio calculated as a function of R_{ch} using Eq. (75). (b) Notations are the same as in (a) but for $N = 4$.

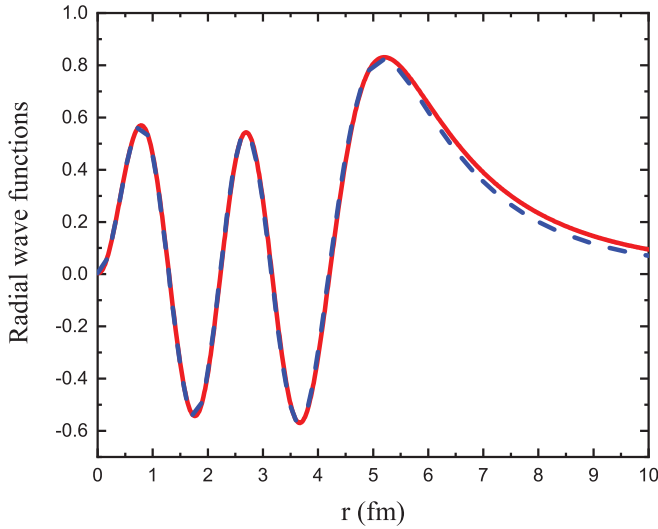


FIG. 9. The solid red line is the $(\alpha^{13}\text{N})_{1/2^+}$ resonance wave function, and the dashed blue line is the radial wave function of the mirror $(\alpha^{13}\text{C})_{1/2^+}$ bound state. r is the distance between the α particle and the c.m. of the nucleus.

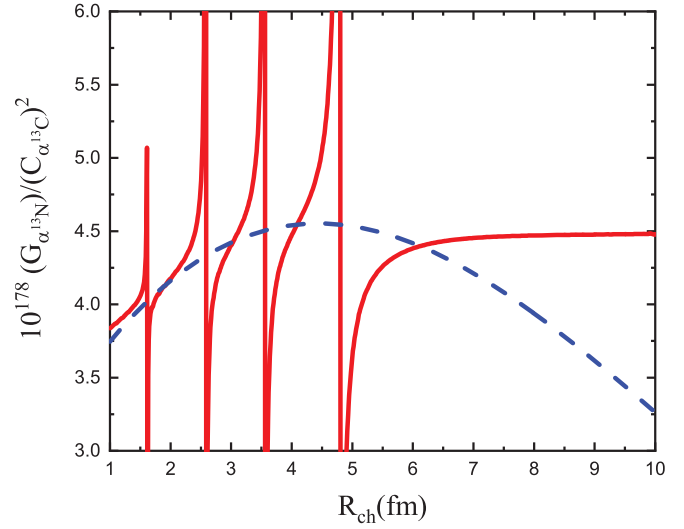


FIG. 10. The $\frac{\Gamma_{\alpha^{13}\text{N}}}{(C_{\alpha^{13}\text{C}})^2}$ ratio for the resonance state $^{17}\text{F}(1/2^+)$ and the mirror bound state $^{17}\text{O}(1/2^+)$: the solid red line is the $\frac{\Gamma_{\alpha^{13}\text{N}}}{(C_{\alpha^{13}\text{C}})^2}$ ratio as a function of R_{ch} calculated using Eq. (72), and the blue dashed line is the $\frac{\Gamma_{\alpha^{13}\text{N}}}{(C_{\alpha^{13}\text{C}})^2}$ ratio calculated as a function of R_{ch} using Eq. (75).

state $^{17}\text{O}(1/2^+)$. The orbital momentum of the mirror states is $l = 1$ and the resonance energy is $E_{\alpha^{13}\text{N}(0)} = 0.7371$ MeV [32]. The location of the state $^{17}\text{O}(1/2^+)$ is questionable. The excitation energy E_x of the state $^{17}\text{O}(1/2^+)$ is 6356 ± 8 keV [32]. Taking into account that the α - ^{13}C threshold is located at 6359.2 keV one finds that this $1/2^+$ level is the located at $E_{\alpha^{13}\text{C}} = -3 \pm 8$ keV; that is, it can be a subthreshold bound state or a resonance [32]. This location of the level $^{17}\text{O}(1/2^+)$ was adopted in the previous analyses of the direct measurements including the latest one in Ref. [33]. If this level is the subthreshold bound state, then its reduced width is related to the ANC of this level. However, in a recent paper [34] it was determined that this level is actually a resonance located at $E_{\alpha^{13}\text{C}} = 4.7 \pm 3$ keV. Because the possible subthreshold state and near threshold resonance are located very close to each other the reduced widths corresponding to these two levels are very close. Here in the analysis I still assume that $^{17}\text{O}(1/2^+)$ is the bound state with the binding energy of -3 keV. I adopt the ANC of this subthreshold state $C_{\alpha^{13}\text{C}}^2 = 4.4 \times 10^{169} \text{ fm}^{-1}$ [35].

The calculated mirror resonance and bound-state wave functions are shown in Fig. 9. They are normalized in the internal region $r \leq 5.2$ fm. Both wave functions are practically identical up to $R_{\text{ch}} \leq 15$ fm.

In Fig. 10 the $\frac{\Gamma_{\alpha^{13}\text{N}}}{(C_{\alpha^{13}\text{C}})^2}$ ratio is calculated using the Wronskian Eq. (72) and the simple Eq. (75). The asymptotic value of the ratio is $\frac{\Gamma_{\alpha^{13}\text{N}}}{(C_{\alpha^{13}\text{C}})^2} = 4.48 \times 10^{-178}$. The value of the $\frac{\Gamma_{\alpha^{13}\text{N}}}{(C_{\alpha^{13}\text{C}})^2}$ at the border of the internal region $R_{\text{ch}} = 5.2$ fm is very close to its asymptotic value. Equation (75) gives $\frac{\Gamma_{\alpha^{13}\text{N}}}{(C_{\alpha^{13}\text{C}})^2} = 4.55 \times 10^{-178}$. Taking into account the adopted value of the ANC $C_{\alpha^{13}\text{C}}$ and the experimental ratio $\frac{\Gamma_{\alpha^{13}\text{N}}}{(C_{\alpha^{13}\text{C}})^2} = 4.48 \times$

10^{-178} one obtains from the Wronskian ratio the resonance width $\Gamma_{\alpha^{13}\text{N}} = 4.48 \times 10^{-178} \times 4.4 \times 10^{169} \times \hbar c = 3.9$ eV.

ACKNOWLEDGMENTS

This work was supported by the U.S. DOE Grant No. DE-FG02-93ER40773, NNSA Grant No. DE-NA0003841, and U.S. NSF Award No. PHY-1415656.

APPENDIX

In this Appendix it is shown that the Zel'dovich regularization procedure can be used for normalization of the resonance wave function $u_{k_p l_B}(r)$ both for exponentially decaying potentials and potentials with the Coulomb tail. The normalization of the resonance wave function depends on its tail. Taking into account Eq. (13) it is enough to consider the integral

$$I(\beta, \nu, z) = \int_0^\infty dr e^{-\beta r^2} e^{zr} r^\nu. \quad (\text{A1})$$

Here, $z = 2ik_{aA(\mathcal{R})}r = 2ik_{aA(0)}r + 2\text{Im}k_{aA(\mathcal{R})}r$. It is assumed that $k_{aA(0)} > \text{Im}k_{aA(\mathcal{R})}$, as it should be for physical resonances. Then $\text{Re}z^2 < 0$. Also

$$\begin{aligned} \nu &= -2i\eta_{aA}^{(\mathcal{R})} = -2i \frac{\gamma}{k_{aA(0)} - i\text{Im}k_{aA(\mathcal{R})}} \\ &= -2i \frac{\gamma k_{aA(0)}}{k_{aA(0)}^2 + (\text{Im}k_{aA(\mathcal{R})})^2} + 2 \frac{\gamma \text{Im}k_{aA(\mathcal{R})}}{k_{aA(0)}^2 + (\text{Im}k_{aA(\mathcal{R})})^2}, \end{aligned} \quad (\text{A2})$$

$\gamma = Z_a Z_A \mu_{aA}/137$. Thus, one can see that for the repulsive Coulomb potential $\text{Re}\nu > 0$ using Eq. (3.462.1) from

769 Ref. [36] one gets

$$I(\beta, \nu, z) = \Gamma(\nu + 1) (2\beta)^{-(\nu+1)/2} e^{z^2/(8\beta)} D_{-\nu-1}(-z/\sqrt{2\beta}). \quad (\text{A3})$$

770 Here $D_\sigma(x)$ is the parabolic cylinder function. For $\text{Re}z^2 < 0$
771 using Eq. (9.246.1) from Ref. [36] one gets

$$I(0, \nu, z) = \lim_{\beta \rightarrow +0} I(\beta, \nu, z) = \Gamma(\nu + 1) (-z)^{-\nu-1}. \quad (\text{A4})$$

772 Thus, the regularization procedure used by Zel'dovich is ap-
773 plicable and for the physical resonances $k_{aA(0)} > \text{Im}k_{aA(\mathcal{R})}$ the
774 integral in Eq. (A1) does exist and converges in $\lim \beta \rightarrow +0$.

Let me consider now the integral

$$I_R(\beta, \nu, z) = \int_R^\infty dr e^{-\beta r^2} e^{zr} r^\nu. \quad (\text{A5})$$

Integrating it by parts one gets

$$\lim_{\beta \rightarrow +0} I_R(\beta, \nu, z) = -\frac{R^\nu}{z} e^{zR} \left[1 - \frac{\nu}{zR} + O\left(\frac{1}{z^2 R^2}\right) \right]. \quad (\text{A6})$$

- [1] L. D. Blokhintsev, I. Borbely, and E. I. Dolinskii, *Fiz. Elem. Chastis At. Yadra* **8**, 1189 (1977) [*Sov. J. Part. Nucl.* **8**, 485 (1977)].
- [2] L. D. Blokhintsev, A. M. Mukhamedzhanov, and A. N. Safronov, *Fiz. Elem. Chastis At. Yadra* **15**, 1296 (1984) [*Sov. J. Part. Nucl.* **15**, 580 (1984)].
- [3] A. M. Mukhamedzhanov and N. K. Timofeyuk, *Pis'ma Zh. Eksp. Teor. Fiz.* **51**, 247 (1990) [*JETP Lett.* **51**, 282 (1990)].
- [4] A. M. Mukhamedzhanov, C. A. Gagliardi, and R. E. Tribble, *Phys. Rev. C* **63**, 024612 (2001).
- [5] A. M. Mukhamedzhanov, L. D. Blokhintsev, and B. F. Irgaziev, *Phys. Rev. C* **83**, 055805 (2011).
- [6] A. M. Mukhamedzhanov and N. K. Timofeyuk, *Yad. Fiz.* **51**, 679 (1990) [*Sov. J. Nucl. Phys.* **51**, 431 (1990)].
- [7] X. Tang, A. Azhari, C. A. Gagliardi, A. M. Mukhamedzhanov, F. Pirlepesov, L. Trache, R. E. Tribble, V. Burjan, V. Kroha, and F. Carstoiu, *Phys. Rev. C* **67**, 015804 (2003).
- [8] A. M. Mukhamedzhanov, M. La Cognata, and V. Kroha, *Phys. Rev. C* **83**, 044604 (2011).
- [9] A. M. Mukhamedzhanov and R. E. Tribble, *Phys. Rev. C* **59**, 3418 (1999).
- [10] N. K. Timofeyuk, R. C. Johnson, and A. M. Mukhamedzhanov, *Phys. Rev. Lett.* **91**, 232501 (2003).
- [11] A. M. Mukhamedzhanov, *Phys. Rev. C* **86**, 044615 (2012).
- [12] R. F. Casten, *Nuclear Structure from a Simple Perspective* (Oxford University Press, New York, 2005).
- [13] H. Kramers, *Hand Jahrb. Chem. Phys.* **1**, 312 (1938).
- [14] W. Heisenberg, *Z. Naturforsch.* **1**, 608 (1946).
- [15] C. Möller, *K. Dan. Vidensk. Selsk. Mat. Fys. Medd.* **22**, 19 (1946).
- [16] N. Hu, *Phys. Rev.* **74**, 131 (1948).
- [17] Ya. B. Zel'dovich, *Zh. Eksp. Teor. Fiz.* **51**, 1492 (1965).
- [18] M. Perelomov, V. S. Popov, and M. V. Terentev, *Zh. Eksp. Teor. Fiz.* **51**, 309 (1966).
- [19] A. M. Lane and R. G. Thomas, *Rev. Mod. Phys.* **30**, 257 (1958).
- [20] W. T. Pinkston and G. R. Satchler, *Nucl. Phys.* **72**, 641 (1965)
- [21] R. J. Philpott, W. T. Pinkston, and G. R. Satchler, *Nucl. Phys. A* **119**, 241 (1968).
- [22] N. K. Timofeyuk, *Nucl. Phys. A* **632**, 19 (1998).
- [23] R. G. Newton, *Scattering Theory of Waves and Particles*, 2nd ed. (Springer-Verlag, Heidelberg, 1982).
- [24] P. Navratil, J. P. Vary, and B. R. Barrett, *Phys. Rev. C* **62**, 054311 (2000).
- [25] P. Navratil and W. E. Ormand, *Phys. Rev. C* **68**, 034305 (2003).
- [26] S. Quaglioni and P. Navratil, *Phys. Rev. Lett.* **101**, 092501 (2008).
- [27] O. Jensen, G. Hagen, M. Hjorth-Jensen, B. A. Brown, and A. Gade, *Phys. Rev. Lett.* **107**, 032501 (2011).
- [28] N. K. Timofeyuk, *Phys. Rev. C* **84**, 054313 (2011).
- [29] F. Ajzenberg-Selove, *Nucl. Phys. A* **523**, 1 (1991).
- [30] Z. H. Liu, C. J. Lin, H. Q. Zhang, Z. C. Li, J. S. Zhang, Y. W. Wu, F. Yang, M. Ruan, J. C. Liu, S. Y. Li, and Z. H. Peng, *Phys. Rev. C* **64**, 034312 (2001).
- [31] N. Imai *et al.*, *Nucl. Phys. A* **688**, 281c (2001).
- [32] D. R. Tilley, H. R. Weller, and C. M. Cheves, *Nucl. Phys. A* **564**, 1 (1993).
- [33] M. Heil, R. Detwiler, R. E. Azuma, A. Couture, J. Daly, J. Görres, F. Käppeler, R. Reifarth, P. Tischhauser, C. Ugalde, and M. Wiescher, *Phys. Rev. C* **78**, 025803 (2008).
- [34] T. Faestermann, P. Mohr, R. Hertenberger, and H.-F. Wirth, *Phys. Rev. C* **92**, 052802(R) (2015).
- [35] A. M. Mukhamedzhanov, Shubhchintak, and C. A. Bertulani, *Phys. Rev. C* **96**, 024623 (2017).
- [36] I. S. Gradshteyn and L. M. Ryzhik, *Tables of Integrals, Series and Products* (Academic Press, New York, 1980).